3
Modelling of Stagewise Processes

3.1
Introduction

The principle of the perfectly-mixed stirred tank has been discussed previously in Section 1.2.2, and this provides an essential building block for modelling applications. In this section, the concept is applied to tank type reactor systems and stagewise mass transfer applications, such that the resulting model equations often appear in the form of linked sets of first-order difference differential equations. Solution by digital simulation works well for small problems, in which the number of equations are relatively small and where the problem is not compounded by stiffness or by the need for iterative procedures. For these reasons, the dynamic modelling of the continuous distillation columns in this section is intended only as a demonstration of method, rather than as a realistic attempt at solution. For the solution of complex distillation and extraction problems, the reader is referred to commercial dynamic simulation packages.

3.2
Stirred-Tank Reactors

3.2.1
Reactor Configurations

This section is concerned with batch, semi-batch, continuous stirred tanks and continuous stirred-tank-reactor cascades, as represented in Fig. 3.1. Tubular chemical reactor systems are discussed in Chapter 4.

Three modes of reactor operation may be distinguished: batch, semi-batch and continuous. In a batch system all reactants are added to the tank at the given starting time. During the course of reaction, the reactant concentrations decrease continuously with time, and products are formed. On completion of the reaction, the reactor is emptied, cleaned and is made ready for another batch and allows differing reactions to be carried out in the same reactor. The disadvantages are the downtime needed for loading and cleaning and possibly the changing reaction conditions. Batch operation is often ideal for small scale flex-

Chemical Engineering Dynamics: An Introduction to Modelling and Computer Simulation, Third Edition
J. Ingham, I. J. Dunn, E. Heinzle, J. E. Prenosil, J. B. Snape

ISBN: 978-3-527-31678-6

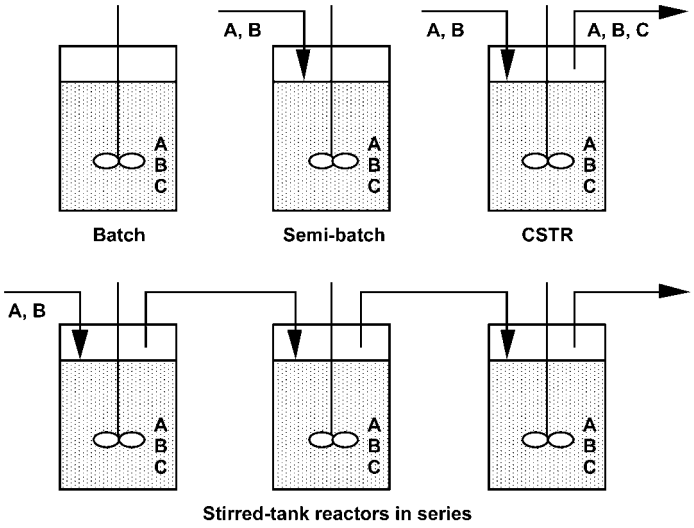

Fig. 3.1 Stirred-tank reactor configurations.

ible production and high value, low output product production, where the chemistry and reaction kinetics are not known exactly.

In many reactions pure batch operation is not possible, mainly due to safety or selectivity reasons. In semi-batch operation, one reactant may be charged to the vessel at the start of the batch, and then the others fed to the reactor at perhaps varying rates and over differing time periods. When the vessel is full, feeding is stopped and the contents allowed to discharge. Semi-batch operation allows one to vary the reactant concentration to a desired level in a very flexible way, and thus to control the reaction rates and the reactor temperature. It is, however, necessary to develop an appropriate feeding strategy. Modelling and simulation allows estimation of optimal feeding profiles. Sometimes it is necessary to adjust the feeding rates using feed-back control. The flexibility of operation is generally similar to that of a batch reactor system.

Continuous operation provides high rates of production with more constant product quality. There are no downtimes during normal operation. Reactant preparation and product treatment also have to run continuously. This requires careful flow control. Continuous operation can involve a single stirred tank, a series of stirred tanks or a tubular-type of reactor. The latter two instances give concentration profiles similar to those of batch operation, whereas in a single stirred tank, the reaction conditions are at the lowest reactant concentration, corresponding to effluent conditions.

3.2.2 Generalised Model Description

The energy and material balance equations for reacting systems follow the same principles, as described previously in Sections 1.2.3 to 1.2.5.

3.2.2.1 Total Material Balance Equation

It becomes necessary to incorporate a total material balance equation into the reactor model, whenever the total quantity of material in the reactor varies, as in the cases of semi-continuous or semi-batch operation or where volume changes occur, owing to density changes in flow systems. Otherwise the total material balance equation can generally be neglected.

The dynamic total material balance equation is represented by

$$\begin{pmatrix}\text{Rate of accumulation}\\ \text{of total mass in system}\end{pmatrix} = \begin{pmatrix}\text{Mass flow rate}\\ \text{into the system}\end{pmatrix} - \begin{pmatrix}\text{Mass flow rate}\\ \text{out of the system}\end{pmatrix}$$

3.2.2.2 Component Balance Equation

The general component balance for a well-mixed tank reactor or reaction region can be written as

$$\begin{pmatrix}\text{Rate of}\\ \text{accumulation}\\ \text{of component}\\ \text{in the}\\ \text{system}\end{pmatrix} = \begin{pmatrix}\text{Rate of}\\ \text{flow of}\\ \text{component}\\ \text{into}\\ \text{the system}\end{pmatrix} - \begin{pmatrix}\text{Rate of}\\ \text{flow of}\\ \text{component}\\ \text{from}\\ \text{the system}\end{pmatrix} + \begin{pmatrix}\text{Rate of}\\ \text{production of}\\ \text{component}\\ \text{by reaction}\end{pmatrix}$$

For batch reactors, there is no flow into or out of the system, and those terms in the component balance equation are therefore zero.

For semi-batch reactors, there is inflow but no outflow from the reactor and the outflow term in the above balance equation is therefore zero.

For steady-state operation of a continuous stirred-tank reactor or continuous stirred-tank reactor cascade, there is no change in conditions with respect to time, and therefore the accumulation term is zero. Under transient conditions, the full form of the equation, involving all four terms, must be employed.

3.2.2.3 Energy Balance Equation

For reactions involving heat effects, the total and component material balance equations must be coupled with a reactor energy balance equation. Neglecting work done by the system on the surroundings, the energy balance is expressed by where each term has units of kJ/s. For steady-state operation the accumulation

$$\begin{pmatrix}\text{Rate of}\\ \text{accumulation}\\ \text{of energy in}\\ \text{the reactor}\end{pmatrix} = \begin{pmatrix}\text{Flow of}\\ \text{energy into}\\ \text{the reactor}\\ \text{in the feed}\end{pmatrix} - \begin{pmatrix}\text{Flow of}\\ \text{energy from}\\ \text{the reactor}\\ \text{in the outlet}\end{pmatrix} + \begin{pmatrix}\text{Rate of}\\ \text{heat transfer}\\ \text{to the}\\ \text{reactor}\end{pmatrix}$$

term is zero and can be neglected. A detailed explanation of energy balancing is found in Section 1.2.5, together with a case study for a reactor.

Both flow terms are zero for the case of batch reactor operation, and the outflow term is zero for semi-continuous or semi-batch operation.

The information flow diagram for a non-isothermal, continuous-flow reactor (in Fig. 1.18, shown previously in Section 1.2.5) illustrates the close interlinking and highly interactive nature of the total material balance, component material balance, energy balance, rate equation, Arrhenius equation and flow effects F. This close interrelationship often brings about highly complex dynamic behaviour in chemical reactors.

3.2.2.4 **Heat Transfer to and from Reactors**

Heat transfer is usually affected by coils or jackets, but can also be achieved by the use of external loop heat exchangers and, in certain cases, heat is transported out of the reactor by the vaporization of volatile material from the reactor. The treatment here mainly concerns jackets and coils. Other examples of heat transfer are illustrated in the simulation examples of Chapter 5.

Figure 3.2 shows the case of a jacketed, stirred-tank reactor, in which either heating by steam or cooling medium can be applied to the jacket. Here V is volume, c_p is specific heat capacity, ρ is density, Q is the rate of heat transfer, U is the overall

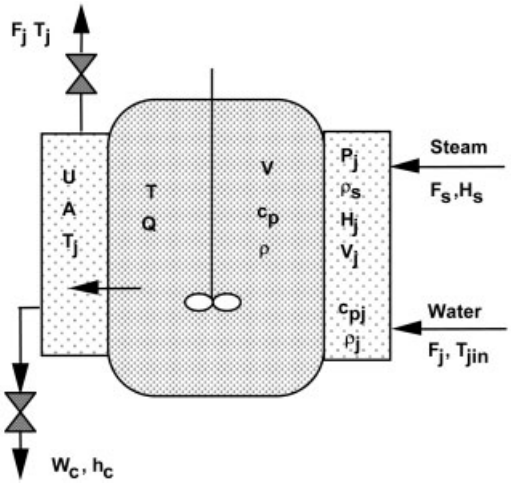

Fig. 3.2 Model representation of a stirred-tank reactor with heat transfer to the jacket.

heat transfer coefficient, A is the area for heat transfer, T is temperature, H is enthalpy of vapour, h is liquid enthalpy, F is volumetric flow rate and W is mass flow rate. The subscripts are j for the jacket, s for steam and c for condensate.

The rate of heat transfer is most conveniently expressed in terms of an overall heat transfer coefficient, the effective area for heat transfer and an overall temperature difference, or driving force, where

$$Q = UA(T - T_j) \quad kJ/s$$

Jacket or Coil Cooling

In simple cases the jacket or cooling temperature, T_j, may be assumed to be constant. In more complex dynamic problems, however, it may be necessary to allow for the dynamics of the cooling jacket, in which case T_j becomes a system variable. The model representation of this is shown in Fig. 3.3.

Under conditions, where the reactor and the jacket are well insulated and heat loss to the surroundings and mechanical work effects may be neglected

$$\begin{pmatrix}\text{Rate of}\\ \text{accumulation}\\ \text{of energy}\\ \text{in the jacket}\end{pmatrix} = \begin{pmatrix}\text{Rate of}\\ \text{energy flow}\\ \text{to the jacket}\\ \text{by convection}\end{pmatrix} - \begin{pmatrix}\text{Rate of}\\ \text{energy flow}\\ \text{from the jacket}\\ \text{by convection}\end{pmatrix} + \begin{pmatrix}\text{Rate of}\\ \text{heat transfer}\\ \text{into}\\ \text{the jacket}\end{pmatrix}$$

or

$$\begin{pmatrix}\text{Rate of}\\ \text{accumulation}\\ \text{of enthalpy}\\ \text{in the jacket}\end{pmatrix} = \begin{pmatrix}\text{Energy}\\ \text{required to}\\ \text{heat coolant}\\ \text{from } T_{jin} \text{ to } T_j\end{pmatrix} + \begin{pmatrix}\text{Rate of}\\ \text{heat transfer}\\ \text{from}\\ \text{the jacket}\end{pmatrix}$$

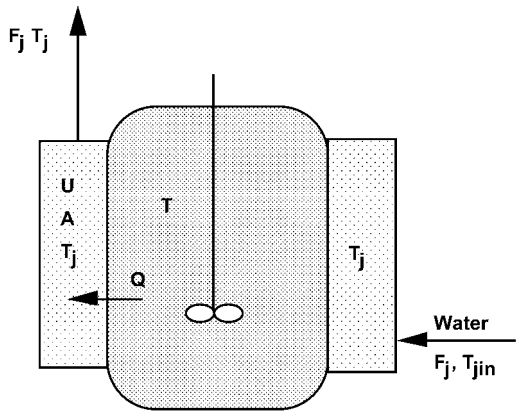

Fig. 3.3 Dynamic model representation of the cooling jacket.

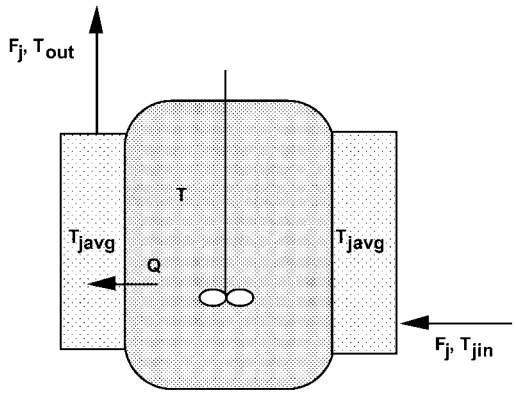

Fig. 3.4 Steady-state model representation of the cooling jacket.

Assuming the liquid in the jacket is well-mixed, the heat balance equation for the jacket becomes

$$V_j \rho_j c_{pj} \frac{dT_j}{dt} = F_j \rho_j c_{pj} (T_{jin} - T_j) + UA(T - T_j)$$

Here F_j is the volumetric flow of coolant to the jacket, T_{jin} is the inlet coolant temperature, and T_j is the jacket temperature. Under well-mixed conditions, T_j is identical to the temperature of the outlet flow.

Alternatively neglecting the jacket dynamics and assuming that the coolant in the jacket is at some mean temperature, T_{javg}, as shown in Fig. 3.4, a steady-state energy balance can be formulated as

$$\begin{pmatrix} \text{Rate of energy gain} \\ \text{by coolant flow} \end{pmatrix} = \begin{pmatrix} \text{Rate of energy transfer} \\ \text{from the reactor to the jacket} \end{pmatrix}$$

$$F_j \rho_j c_{pj} (T_{jout} - T_{jin}) = UA(T - T_{javg}) = Q$$

Assuming an arithmetic mean jacket temperature,

$$T_{javg} = \frac{T_{jin} + T_{jout}}{2}$$

Substituting for T_{jout} into the steady-state jacket energy balance, solving for T_{javg} and substituting T_{javg} into the steady-state balance, gives the result that

$$Q = UAK_1 (T - T_{jin})$$

where K_1 is given by

$$K_1 = \frac{2F_j\rho_j c_{pj}}{UA + 2F_j\rho_j c_{pj}}$$

As shown in several of the simulation examples, the fact that Q is now a function of the flow rate, F_j, provides a convenient basis for the modelling of cooling effects, and control of the temperature of the reactor by regulation of the flow of coolant.

3.2.2.5 **Steam Heating in Jackets**

The dynamics of the jacket are more complex for the case of steam heating. The model representation of the jacket steam heating process is shown in Fig. 3.5.

A material balance on the steam in the jacket is represented by

$$\begin{pmatrix}\text{Rate of}\\ \text{accumulation}\\ \text{of steam}\\ \text{in the jacket}\end{pmatrix} = \begin{pmatrix}\text{Mass flow}\\ \text{of steam}\\ \text{to the}\\ \text{jacket}\end{pmatrix} - \begin{pmatrix}\text{Mass flow of}\\ \text{condensate}\\ \text{from the}\\ \text{jacket}\end{pmatrix}$$

$$V_j\frac{d\rho_j}{dt} = F_s\rho_s - W_c$$

The enthalpy balance on the jacket is given by

$$V_j\frac{d(H_j\rho_j)}{dt} = F_s\rho_s H_s + UA(T - T_j) - W_c H_c$$

where H_j is the enthalpy of the steam in the jacket.

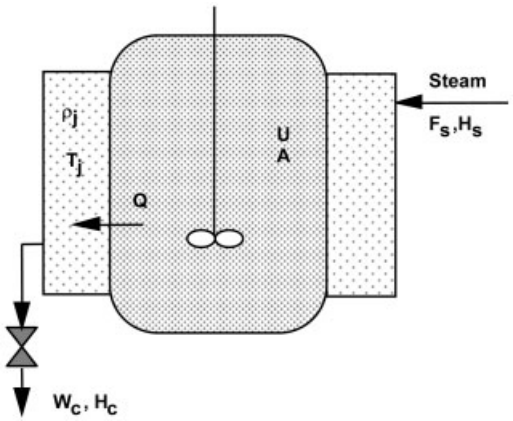

Fig. 3.5 Model representation of steam heating in the jacket.

The saturated steam density, ρ_j, depends on the jacket temperature, T_j, in the first approximation in accordance with the Ideal Gas Law and hence

$$\rho_j = \frac{18P_j}{RT_j}$$

where R is the Ideal Gas Constant.

The jacket steam pressure, P_j, is itself a function of the jacket steam temperature, T_j, as listed in steam tables or as correlated by the Antoine equation for vapour pressure, where

$$P_j = \exp\left(\frac{A}{T_j} + B\right)$$

Here, A and B are the Antoine steam constants and T_j is the absolute steam temperature.

Combining the two equations for steam density and pressure gives an implicit equation requiring a numerical root estimation.

$$0 = P_j - \exp\left(\frac{A}{18P_j/R\rho_j} + B\right)$$

The MADONNA root finder provides a powerful means of solution. An example of the use of root finder is employed in the simulation example RELUY for steam jacket dynamics. Other examples of use are in BUBBLE and STEAM.

3.2.2.6 **Dynamics of the Metal Jacket Wall**

In some cases, where the wall of the reactor has an appreciable thermal capacity, the dynamics of the wall can be of importance (Luyben, 1973). The simplest approach is to assume the whole wall material has a uniform temperature and therefore can be treated as a single lumped parameter system or, in effect, as a single well-stirred tank. The heat flow through the jacket wall is represented in Fig. 3.6.

The nomenclature is as follows: Q_m is the rate of heat transfer from the reactor to the reactor wall, Q_j is the rate of heat transfer from the reactor wall to the jacket, and

$$Q_m = U_m A_m (T - T_m)$$

$$Q_j = U_j A_j (T_m - T_j)$$

Here, U_m is the film heat transfer coefficient between the reactor and the reactor wall. U_j is the film heat transfer coefficient between the reactor wall and the jacket. A_m is the area for heat transfer between the reactor and the wall. A_j is the area for heat transfer between the wall and the jacket.

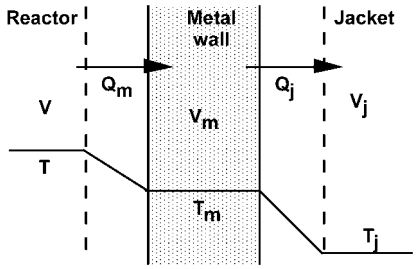

Fig. 3.6 Model representation of heat flow through a reactor wall with assumed uniform temperature.

The heat balance for the wall gives

$$V_m \rho_m c_{pm} \frac{dT_m}{dt} = Q_m - Q_j$$

and the balance for the jacket becomes

$$V_j \rho_j c_{pj} \frac{dT_j}{dt} = F_j \rho_j c_{pj} (T_{jin} - T_j) + Q_j$$

In some cases, it may be of interest to model the temperature distribution through the wall.

This might be done by considering the metal wall and perhaps also the jacket as consisting of a series of separate regions of uniform temperature, as shown in Fig. 3.7. The balances for each region of metal wall and cooling water volume then become for any region, n

$$V_{mn} \rho_m c_{pm} \frac{dT_{mn}}{dt} = Q_{mn} - Q_{jn}$$

$$V_{jn} \rho_j c_{pj} \frac{dT_{jn}}{dt} = F_j \rho_j c_{pj} (T_{jn-1} - T_{jn}) + Q_{jn}$$

where V_{mn} and V_{jn} are the respective volumes of the wall and coolant in element n. A_{mn} and A_{jn} are the heat transfer areas for transfer from the reactor to the wall and from the wall to the jacket. Hence:

$$Q_{mn} = U_m A_{mn} (T - T_{mn})$$

$$Q_{jn} = U_j A_{jn} (T_{mn} - T_{jn})$$

Note that the effects of thermal conduction along the jacket wall are assumed to be negligible in this case.

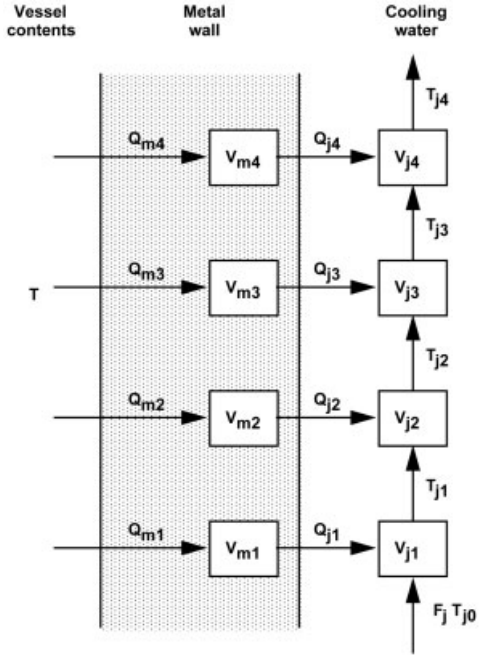

Fig. 3.7 Model representation of temperature distribution in the wall and jacket, showing wall and jacket with four lumped parameters.

3.2.3
The Batch Reactor

It is assumed that all the tank-type reactors, covered in this and the immediately following sections, are at all times perfectly mixed, such that concentration and temperature conditions are uniform throughout the tanks contents. Figure 3.8 shows a batch reactor with a cooling jacket. Since there are no flows into the reactor or from the reactor, the total material balance tells us that the total mass, within the reactor, remains constant.

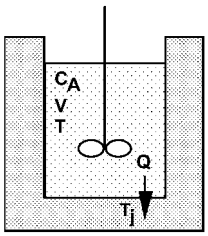

Fig. 3.8 The batch reactor with heat transfer.

Component Balance Equation

$$\begin{pmatrix}\text{Rate of accumulation}\\ \text{of reactant A}\end{pmatrix} = \begin{pmatrix}\text{Rate of production of A}\\ \text{by chemical reaction}\end{pmatrix}$$

Thus,

$$\frac{dn_A}{dt} = r_A V$$

or since

$$n_A = n_{A0}(1 - X_A)$$

$$n_{A0}\frac{dX_A}{dt} = -r_A V$$

or for constant volume

$$C_{A0}\frac{dX_A}{dt} = -r_A$$

Energy Balance Equation

$$\begin{pmatrix}\text{Rate of}\\ \text{accumulation}\\ \text{of heat in}\\ \text{the reactor}\end{pmatrix} = \begin{pmatrix}\text{Rate of heat}\\ \text{generation}\\ \text{by reaction}\end{pmatrix} - \begin{pmatrix}\text{Rate of heat}\\ \text{transfer to}\\ \text{the surroundings}\end{pmatrix}$$

$$V\rho c_p\frac{dT}{dt} = Vr_Q - UA(T - T_j)$$

Here V is the volume of the reactor, ρ is the density, c_p is the mean specific heat of the reactor contents (kJ/kg K) and r_Q is the rate of generation of heat by reaction (kJ/s m^3).

3.2.3.1 Case A: Constant-Volume Batch Reactor

A constant volume batch reactor is used to convert reactant, A, to product, B, via an endothermic reaction, with simple stoichiometry, $A \rightarrow B$. The reaction kinetics are second-order with respect to A, thus

$$r_A = -kC_A^2$$

From the reaction stoichiometry, product B is formed at exactly the same rate as that at which reactant A is decomposed.

The rate equation with respect to A is

$$-r_A = kC_A^2 = kC_{A0}^2(1 - X_A)^2$$

giving the component balance equation as

$$\frac{dX_A}{dt} = kC_{A0}(1 - X_A)^2$$

For the second-order reaction, the term representing the rate of heat production by reaction simplifies to

$$r_Q V = -r_A(-\Delta H)V = kC_{A0}^2(1 - X_A)^2(-\Delta H)V$$

This gives the resultant heat balance equation as

$$V\rho c_p \frac{dT}{dt} = kC_{A0}^2(1 - X_A)^2(-\Delta H)V + UA(T_j - T)$$

where it is assumed that heat transfer to the reactor occurs via a coil or jacket heater.

The component material balance, when coupled with the heat balance equation and temperature dependence of the kinetic rate coefficient, via the Arrhenius relation, provide the dynamic model for the system. Batch reactor simulation examples are provided by BATCHD, COMPREAC, BATCOM, CASTOR, HYDROL and RELUY.

3.2.4
The Semi-Batch Reactor

A semi-batch reactor with one feed stream and heat transfer to a cooling jacket is shown in Fig. 3.9.

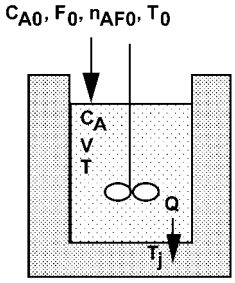

Fig. 3.9 The semi-batch reactor.

Total Material Balance

A total material balance is necessary, owing to the feed input to the reactor, where

$$\begin{pmatrix}\text{Rate of accumulation}\\ \text{of mass in the reactor}\end{pmatrix} = \begin{pmatrix}\text{Mass flow}\\ \text{rate in}\end{pmatrix}$$

$$\frac{d(\rho V)}{dt} = F_0\rho_0$$

Here ρ_0 is the feed density.

The density in the reactor, ρ, may be a function of the concentration and temperature conditions within the reactor. Assuming constant density conditions

$$\frac{dV}{dt} = F$$

Component Balance Equation

All important components require a component balance.

For a given reactant A

$$\begin{pmatrix}\text{Rate of}\\ \text{accumulation of A}\end{pmatrix} = \begin{pmatrix}\text{Rate of flow}\\ \text{of A in}\end{pmatrix} + \begin{pmatrix}\text{Rate of production}\\ \text{of A by reaction}\end{pmatrix}$$

$$\frac{dn_A}{dt} = N_{A0} + r_A V$$

where N_{A0} is the molar feeding rate of A per unit time.

In terms of concentration, this becomes

$$\frac{d(VC_A)}{dt} = F_0 C_{A0} + r_A V$$

where F is the volumetric feed rate and C_{A0} is the feed concentration. Note that both the volumetric flow and the feed concentration can vary with time, depending on the particular reactor feeding strategy.

Energy Balance Equation

Whenever changes in temperature are to be calculated, an energy balance is needed. With the assumption of constant c_p and constant ρ, as derived in Section 1.2.5, the balance becomes

$$\rho c_p V\frac{dT}{dt} = F_0\rho c_p(T_0 - T) + r_Q V + Q$$

Note that the available heat transfer area may also change as a function of time, and may therefore also form an additional variable in the solution. Note also that although constant ρ and c_p have been assumed here, this is not a restrictive condition and that equations showing the variations of these properties are easily included in any simulation model.

3.2.4.1 Case B: Semi-Batch Reactor

A semi-batch reactor is used to convert reactant, A, to product, B, by the reaction $A \rightarrow 2B$. The reaction is carried out adiabatically. The reaction kinetics are as before

$$r_A = -kC_A^2$$

and the stoichiometry gives

$$r_B = -2r_A = +2kC_A^2$$

The balances for the two components A and B, with flow of A, into the reactor are now

$$\frac{d(VC_A)}{dt} = FC_{A0} + r_A V$$

$$\frac{d(VC_B)}{dt} = r_B V$$

and the enthalpy balance equation is

$$V\rho c_p \frac{dT}{dt} = F\rho c_p (T_0 - T) + kC_{A0}^2 (1 - X_A)^2 (-\Delta H_A) V$$

since, for adiabatic operation, the rate of heat input into the system, Q, is zero.

With initial conditions for the initial molar quantities of A and B (VC_A, VC_B), the initial temperature, T, and the initial volume of the contents, V, specified, the resulting system of equations can be solved to obtain the time-varying quantities, V(t), $VC_A(t)$, $VC_B(t)$, T(t) and hence also concentrations C_A and C_B as functions of time. Examples of semi-batch operations are given in the simulation examples HMT, SEMIPAR, SEMISEQ, RUN, SULFONATION and SEMIEX.

3.2.5 The Continuous Stirred-Tank Reactor

Although continuous stirred-tank reactors (Fig. 3.10) normally operate at steady-state conditions, a derivation of the full dynamic equation for the system is nec-

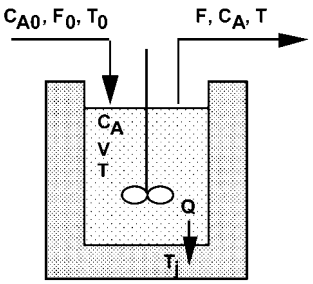

Fig. 3.10 Continuous stirred-tank reactor with heat transfer.

essary to cover the instances of plant start up, shut down and the application of reactor control.

Total Material Balance

The dynamic total material balance equation is given by

$$\begin{pmatrix}\text{Rate of accumulation}\\ \text{of mass in the reactor}\end{pmatrix} = \begin{pmatrix}\text{Mass flow}\\ \text{rate in}\end{pmatrix} - \begin{pmatrix}\text{Mass flow}\\ \text{rate out}\end{pmatrix}$$

$$\frac{dV}{dt} = F_0\rho_0 - F\rho$$

Under constant volume and constant density conditions

$$\frac{dV}{dt} = F_0 - F = 0$$

and therefore

$$F_0 = F$$

Component Material Balance Equation

The component material balance equation is given by

$$\begin{pmatrix}\text{Rate of}\\ \text{accumulation}\\ \text{of component}\\ \text{in the reactor}\end{pmatrix} = \begin{pmatrix}\text{Rate of}\\ \text{flow in of}\\ \text{component}\end{pmatrix} - \begin{pmatrix}\text{Rate of}\\ \text{flow out of}\\ \text{component}\end{pmatrix} + \begin{pmatrix}\text{Rate of}\\ \text{production of}\\ \text{component}\\ \text{by reaction}\end{pmatrix}$$

For a given reactant A

$$\frac{dn_A}{dt} = N_{A0} - N_A - r_A V$$

where n_A is the moles of A in the reactor, N_{A0} is the molar feeding rate of A to the reactor, and N_A is the molar flow rate of A from the reactor.

Under constant density and constant volume conditions, this may be expressed as

$$V\frac{dC_A}{dt} = FC_{A0} - FC_A + r_A V$$

or

$$\frac{dC_A}{dt} = \frac{C_{A0} - C_A}{\tau} + r_A$$

where τ (=V/F) is the average holdup time or residence time of the reactor.

For steady-state conditions to be maintained, the volumetric flow rate F and inlet concentration C_{A0} must remain constant and

$$\frac{dC_A}{dt} = 0$$

hence at steady state

$$r_A V = -F(C_{A0} - C_A) = -(N_{A0} - N_A)$$

and

$$X_A = \frac{N_{A0} - N_A}{N_{A0}} = -\frac{r_A V}{N_{A0}} = -\frac{r_A V}{FC_{A0}}$$

or

$$\tau = \frac{V}{F} = \frac{C_{A0}X_A}{r_A}$$

Energy Balance Equation

This, like the other dynamic balances for the CSTR, follows the full generalised form, of Section 1.2.5, giving

$$\begin{pmatrix}\text{Rate of}\\ \text{accumulation}\\ \text{of energy in}\\ \text{the reactor}\end{pmatrix} = \begin{pmatrix}\text{Energy needed}\\ \text{to heat the}\\ \text{feed to outlet}\\ \text{temperature}\end{pmatrix} + \begin{pmatrix}\text{Rate of}\\ \text{generation}\\ \text{of heat by}\\ \text{reaction}\end{pmatrix} + \begin{pmatrix}\text{Rate of}\\ \text{heat transfer}\\ \text{from the}\\ \text{surroundings}\end{pmatrix}$$

or assuming constant c_p

$$V\rho c_p\frac{dT}{dt} = F_0\rho c_p(T_0 - T) + r_Q V + Q$$

3.2.5.1 Case C: Constant-Volume Continuous Stirred-Tank Reactor

The chemical reaction data are the same as in the preceding example. The reaction kinetics are

$$r_A = -kC_A^2$$

with

$$r_B = -2r_A$$

and the component balances for both A and B are given by

$$V\frac{dC_A}{dt} = FC_{A0} - FC_A + r_A V$$

$$V\frac{dC_B}{dt} = FC_{B0} - FC_B + r_B V$$

Assuming both constant density and constant specific heat, the heat balance equation becomes

$$V\rho c_p\frac{dT}{dt} = F\rho c_p(T_0 - T) + kC_A^2 V(-\Delta H) - UA(T - T_j)$$

Here cooling of an exothermic chemical reaction, via a cooling coil or jacket, is included.

3.2.6 Stirred-Tank Reactor Cascade

For any continuous stirred-tank reactor, n, in a cascade of reactors (Fig. 3.11) the reactor n receives the discharge from the preceding reactor, n – 1, as its feed and discharges its effluent into reactor n + 1, as feed to that reactor.

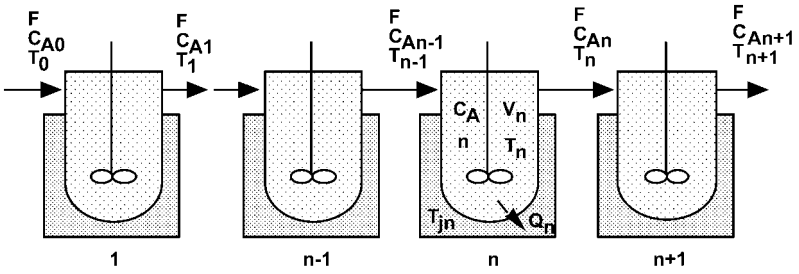

Fig. 3.11 Cascade of continuous stirred-tank reactors.

Thus the balance equations for reactor, n, simply become

$$V_n \frac{dC_{An}}{dt} = FC_{An-1} - FC_{An} + r_{An}V_n$$

$$V_n \rho c_p \frac{dT_n}{dt} = F\rho c_p(T_{n-1} - T_n) + r_{Qn}V + Q_n$$

where, for example,

$$r_{An} = -k_n C_{An}^{\alpha} C_{Bn}^{\beta}$$

$$k_n = Ze^{-E/RT_n}$$

and

$$Q_n = U_n A_n (T_{jn} - T_n)$$

Thus the respective rate expressions depend upon the particular concentration and temperature levels that exist within reactor n. The rate of production of heat by reaction r_Q was defined in Section 1.2.5 and includes all occurring reactions. Simulation examples pertaining to stirred tanks in series are CSTRPULSE, CASCSEQ and COOL.

3.2.7 Reactor Stability

Consider a simple first-order exothermic reaction, $A \rightarrow B$, carried out in a single, constant-volume, continuous stirred-tank reactor (Fig. 3.10), with constant jacket coolant temperature, where $r_A = kC_A$.

The model equations are then given by

$$V\frac{dC_A}{dt} = F(C_{A0} - C_A) - VkC_A$$

$$V\rho c_p \frac{dT}{dt} = F\rho c_p(T_0 - T) + VkC_A(-\Delta H) - UA(T - T_j)$$

$$k = Ze^{-E/RT}$$

At steady state, the temperature and concentration in the reactor are constant with respect to time and

$$\frac{dC_A}{dt} = \frac{dT}{dt} = 0$$

Hence from the component material balance

$$F(C_{A0} - C_A) = VkC_A$$

the steady-state concentration is given by

$$C_A = \frac{C_{A0}}{1 + kV/F}$$

From the steady-state heat balance the heat losses can be equated to the heat gained by reaction, giving

$$-F\rho c_p(T_0 - T) + UA(T - T_j) = VkC_A(-\Delta H) = \frac{VkC_{A0}(\Delta H)}{1 + kV/F}$$

i.e.,

$$\begin{pmatrix} \text{Net rate of} \\ \text{heat loss from} \\ \text{the reactor} \end{pmatrix} = \begin{pmatrix} \text{Rate of heat generation} \\ \text{by chemical reaction in} \\ \text{the reactor} \end{pmatrix}$$

or

$$H_L = H_G$$

The above equation then represents the balanced conditions for steady-state reactor operation. The rate of heat loss, H_L, and the rate of heat gain, H_G, terms may be calculated as functions of the reactor temperature. The rate of heat loss, H_L, plots as a linear function of temperature, and the rate of heat gain, H_G, owing to the exponential dependence of the rate coefficient on temperature, plots as a sigmoidal curve, as shown in Fig. 3.12. The points of intersection of the rate of heat lost and the rate of heat gain curves thus represent potential steady-

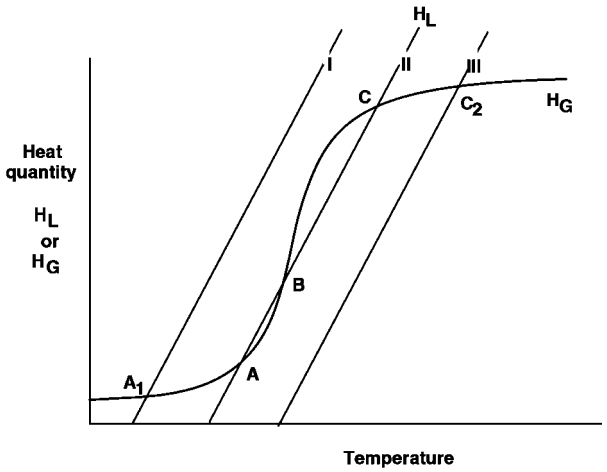

Fig. 3.12 Heat loss H_L and heat gain H_G in a steady-state continuous stirred-tank reactor.

state operating conditions that satisfy the above steady-state heat balance criterion.

Figure 3.12 shows the heat gain curve, H_G, for one particular set of system parameters, and a set of three possible heat loss, H_L, curves. Possible curve intersection points, A_1 and C_2, represent singular stable steady-state operating curves for the reactor, with cooling conditions as given by cooling curves, I and III, respectively.

The cooling conditions given by curve II, however, indicate three potential steady-state solutions at the curve intersections A, B and C. By considering the effect of small temperature variations, about the three steady-state conditions, it can be shown that points A and C represent stable, steady-state operating conditions, whereas the curve intersection point B is unstable. On start up, the reaction conditions will proceed to an eventual steady state, at either point A or at point C. Since point A represents a low temperature, and therefore a low conversion operating state, it may be desirable that the initial transient conditions in the reactor should eventually lead to C, rather than to A. However if point C is at a temperature which is too high and might possibly lead to further decomposition reactions, then A would be the desired operating point.

The basis of the argument for intersection point, B, being unstable is as follows and is illustrated in Fig. 3.13.

Consider a small positive temperature deviation, moving to the right of point B. The condition of the reactor is now such that the H_G value is greater than that for H_L. This will cause the reactor to heat up and the temperature to increase further, until the stable steady-state solution at point C is attained. For a small temperature decrease to the left of B, the situation is reversed, and the reactor will continue to cool, until the stable steady-state solution at point A is attained. Similar arguments show that points A and C are stable steady states.

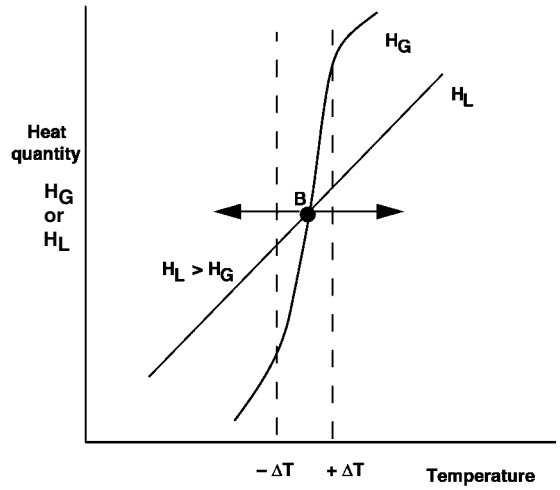

Fig. 3.13 Characteristics of unstable point B of Fig. 3.12.

System stability can also be analysed in terms of the linearised differential model equations. In this, new perturbation variables for concentration C′ and temperature T′ are defined. These are defined in terms of small deviations in the actual reactor conditions away from the steady-state concentration and temperature C_{ss} and T_{ss} respectively. Thus

$$C' = C - C_{ss} \quad \text{and} \quad T' = T - T_{ss}$$

The linearisation of the non-linear component and energy balance equations, based on the use of Taylor's expansion theorem, leads to two, simultaneous, first-order, linear differential equations with constant coefficients of the form

$$\frac{dC'}{dt} = a_1 C' + b_1 T'$$

$$\frac{dT'}{dt} = a_2 C' + b_2 T'$$

The coefficients of the above equations are the partial differentials of the two dynamic balance equations evaluated at C_{ss}, T_{ss} and are given by

$$a_1 = \left|\frac{\partial F(C,T)}{\partial C'}\right|_{C_{ss},T_{ss}}$$

$$b_1 = \left|\frac{\partial F(C,T)}{\partial T'}\right|_{C_{ss},T_s s}$$

$$a_2 = \left|\frac{\partial G(C,T)}{\partial C'}\right|_{C_{ss},T_{ss}}$$

$$b_2 = \left|\frac{\partial G(C,T)}{\partial T'}\right|_{C_{ss},T_{ss}}$$

where F(C, T) represents the dynamic component balance equation and G(C, T) represents the dynamic heat balance equation.

The two linearised model equations have the general solution of the form

$$C' = ae^{\lambda_1 t} + be^{\lambda_2 t}$$

and

$$T' = ce^{\lambda_1 t} + de^{\lambda_2 t}$$

The dynamic behaviour of the system is thus determined by the values of the exponential coefficients, λ_1 and λ_2, which are the roots of the characteristic

equation or eigenvalues of the system and which are also functions of the system parameters.

If λ_1 and λ_2 are real numbers and both have negative values, the values of the exponential terms and hence the magnitudes of the perturbations away from the steady-state conditions, c′ and T′, will reduce to zero with increasing time. The system response will therefore decay back to its original steady-state value, which is therefore a stable steady-state solution or stable node.

If λ_1 and λ_2 are real numbers and both or one of the roots are positive, the system response will diverge with time and the steady-state solution will therefore be unstable, corresponding to an unstable node.

If the roots are, however, complex numbers, with one or two positive real parts, the system response will diverge with time in an oscillatory manner, since the analytical solution is then one involving sine and cosine terms. If both roots, however, have negative real parts, the sine and cosine terms still cause an oscillatory response, but the oscillation will decay with time, back to the original steady-state value, which, therefore remains a stable steady state.

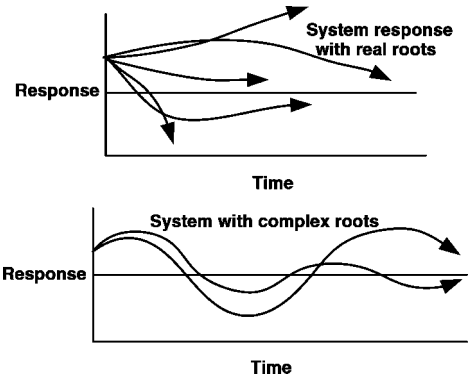

Fig. 3.14 Systems response with real and complex roots.

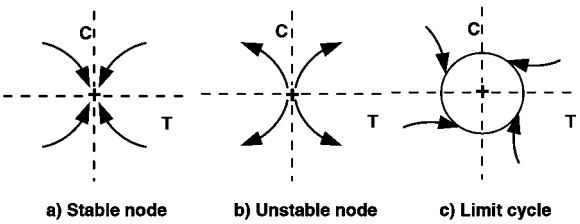

Fig. 3.15 Phase-plane representations of reactor stability. In the above diagrams the point + represents a possible steady-state solution, which (a) may be stable, (b) may be unstable or (c) about which the reactor produces sustained oscillations in temperature and concentration.

If the roots are pure imaginary numbers, the form of the response is purely oscillatory, and the magnitude will neither increase nor decay. The response, thus, remains in the neighbourhood of the steady-state solution and forms stable oscillations or limit cycles.

The types of system behaviour predicted by the above analysis are depicted in Figs. 3.14 and 3.15. The phase-plane plots of Fig. 3.15 give the relation of the dependent variables C and T. Detailed explanation of phase-plane plots is given in control textbooks (e.g., Stephanopoulos, 1984). Linearisation of the reactor model equations is used in the simulation example, HOMPOLY.

Thus it is possible for continuous stirred-tank reactor systems to be stable, or unstable, and also to form continuous oscillations in output, depending upon the system, constant and parameter, values.

This analysis is limited, since it is based on a steady-state criterion. The linearisation approach, outlined above, also fails in that its analysis is restricted to variations, which are very close to the steady state. While this provides excellent information on the dynamic stability, it cannot predict the actual trajectory of the reaction, once this departs from the near steady state. A full dynamic analysis is, therefore, best considered in terms of the full dynamic model equations and this is easily effected, using digital simulation. The above case of the single CSTR, with a single exothermic reaction, is covered by the simulation examples THERMPLOT and THERM. Other simulation examples, covering aspects of stirred-tank reactor stability are COOL, OSCIL, REFRIG1 and REFRIG2. Phase-plane plots are very useful for the analysis of such systems.

3.2.8
Reactor Control

Two simple forms of a batch reactor temperature control are possible, in which the reactor is either heated by a controlled supply of steam to the heating jacket, or cooled by a controlled flow of coolant (Fig. 3.16). Other control schemes

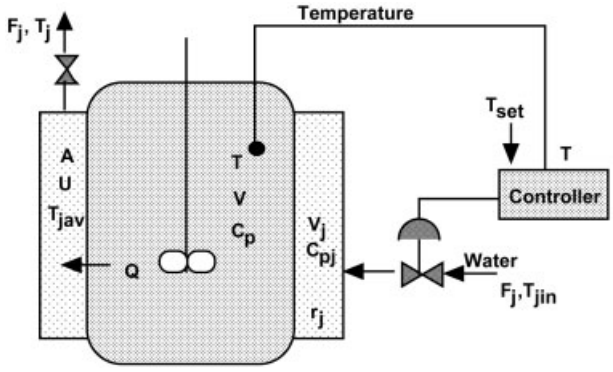

Fig. 3.16 Reactor with control of temperature by manipulating the flow of cooling water.

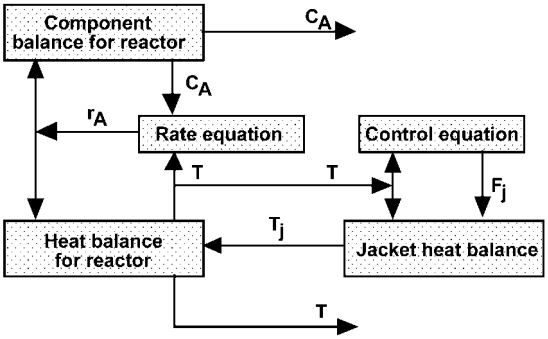

Fig. 3.17 Information flow diagram for the above reactor control implementation.

would be to regulate the reactor flow rate or feed concentration, in order to maintain a given reaction rate (see simulation example SEMIEX).

Figure 3.17 represents an information flow diagram for the above control scheme.

Assuming the jacket is well-mixed, a heat balance on the jacket gives

$$V_j \rho_j c_{pj} \frac{dT_j}{dt} = F_j \rho_j c_{pj} (T_{jin} - T_j) + UA(T - T_j)$$

Consider the case of a proportional controller, which is required to maintain a desired reactor temperature, by regulating the flow of coolant. Neglecting dynamic jacket effects, the reactor heat balance can then be modified to include the effect of the varying coolant flow rate, F_j, in the model equation as:

$$V \rho c_p \frac{dT}{dt} = -r_Q V + UAK_1 (T - T_{jin})$$

where the mean temperature of the jacket is accounted for by the term K_1, as shown in Section 3.2.2.4, and given by

$$K_1 = \frac{2F_j \rho_j c_{pj}}{UA + 2F_j \rho_j c_{pj}}$$

For a proportional controller

$$F_j = F_{jss} + K_c (T - T_{set})$$

where K_c is the proportional gain of the controller and the temperature difference term $(T - T_{set})$, represents the error between the reactor temperature T and controller set point T_{set}. Note that in this conventional negative feedback system, when the reactor temperature, T, is below the setpoint temperature, T_{set}, the coolant flow is decreased, in order to reduce the rate of heat loss from the reactor to the jacket.

Note also that the incorporation of the controller equation and parameter value, K_c, into the dynamic model also alters the stability parameters for the system and thus can also change the resultant system stability characteristics. A stable system may be made to oscillate by the use of high values of K_c or by the use of a positive feedback action, obtained with the use of the controller equation with K_c negative. Thus the reactor acts to provide greater degrees of cooling when $T < T_{set}$, and conversely reduced degrees of cooling when $T > T_{set}$. This phenomenon is shown particularly in simulation example OSCIL.

This example shows that the reactor may oscillate either naturally according to the system parameters or by applied controller action. Owing to the highly non-linear behaviour of the system, it is sometimes found that the net yield from the reactor may be higher under oscillatory conditions than at steady state (see simulation examples OSCIL and COOL). It should be noted also that, under controlled conditions, T_{set} need not necessarily be set equal to the steady-state value T and T_{set}, and that the control action may be used to force the reactor to a more favourable yield condition than that simply determined by steady-state balance considerations.

The proportional and integral controller equation

$$F_j = F_{jss} + K_c\varepsilon + \frac{K_c}{\tau_I}\int_0^t \varepsilon dt$$

where τ_I is the integral time constant and ε is the error = $(T - T_{set})$ or $(C_A - C_{Aset})$ can similarly be incorporated into the reactor simulation model.

Luyben (1973) (see simulation example RELUY) also demonstrates a reactor simulation including the separate effects of the measuring element, measurement transmitter, pneumatic controller and valve characteristics which may in some circumstances be preferable to the use of an overall controller gain term.

3.2.9
Chemical Reactor Safety

A necessary condition for chemical production is the safe operation of chemical reactors and other unit processes (Grewer, 1994). This is best achieved by the design of inherently safe processes, i.e. processes with negligible potential for the release of harmful chemicals. This is often impossible owing to the requirement for active substrates or because of the inherently high reactivity of certain products. The next possible improvement may be made by minimizing the amount of material held under critical conditions or by maintaining process conditions, e.g. pressure and temperature, in the ranges of non-critical conditions. Modeling and simulation provide modern tools for the support of risk analysis and are of major importance for the design of safe chemical reactors and safe operation of chemical reactors (Stoessel, 1995). In the following, safety aspects of batch reactor design and operation are discussed.

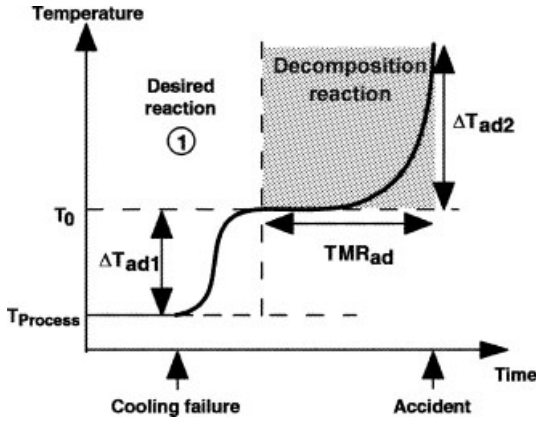

Fig. 3.18 Scenario of cooling failure with thermal runaway. ΔT_{ad1} is the adiabatic temperature rise by desired reaction. ΔT_{ad2} is the adiabatic temperature increase by the decomposition reaction. The time required for this increase is TMR_{ad}.

3.2.9.1 **The Runaway Scenario**

A most critical event for an exothermic chemical reaction is that of a cooling failure. Depending on the reactive potential of the process the temperature of the reactor will rise and may thus possibly trigger the formation of unwanted decomposition reactions with often very large potential for possible reactor failure (Fig. 3.18). The thermal runaway of a polymerisation reaction is described in the simulation example RUN. The reactor operation, i.e. feeding of reactants, the selection of process temperature etc., has to be such that a cooling failure will not cause a reaction runaway or that the time-to-maximum rate criterion, TMR_{ad}, is sufficiently long, e.g. 24 hours, to permit the appropriate safety actions to be taken. See example SULFONATION where substrate feed is adjusted such as to keep TMR_{ad} always above 24 hours. A proper safety assessment should start with calorimetric measurements to allow the estimation of $\Delta T_{ad,2}$, the adiabatic temperature rise by decomposition reaction, and also of the time required for this, TMR_{ad}. This study is preferably achieved via the use of differential scanning calorimetry, DSC.

Other simulation examples involving various safety aspects are HMT, THERM, REFRIG1, REFRIG2 and DSC.

3.2.9.2 **Reaction Calorimetry**

In differential scanning calorimetry, the selected chemical reaction is carried out in a crucible and the temperature difference ΔT compared to that of an empty crucible is measured. The temperature is increased by heating and from the measured ΔT the heat production rate, q, can be calculated (Fig. 3.19). Integration of the value of q with respect to time yields measures of the total heats

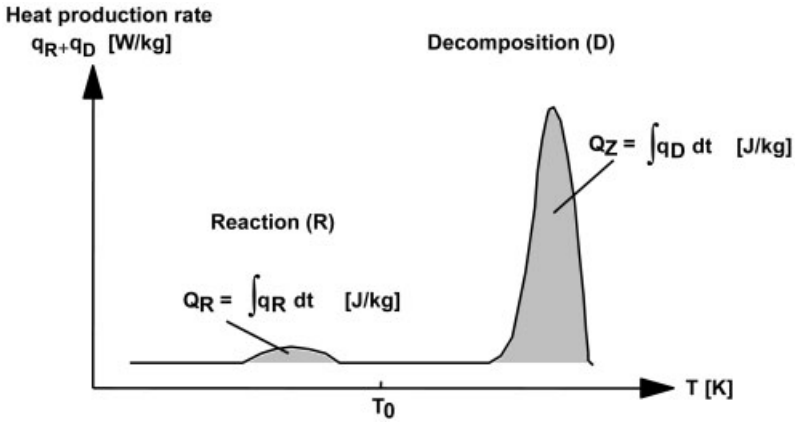

Fig. 3.19 Differential scanning calorimetry with heat release by desired reaction, R and by decomposition reaction D.

released, Q_R, and Q_D, from which ΔH_R and ΔH_D as well as ΔT_{ad1} and ΔT_{ad2} can be calculated from Fig. 3.18. The estimation of the activation energy, E_a, is possible by the use of isothermal DSC based on the following equation

$$q = k_0 f(c)(-\Delta H_R) \exp\left(-\frac{E_a}{RT}\right)$$

or in its logarithmic form

$$\ln q = \ln[k_0 f(c)(-\Delta H_R)] - \frac{E_a}{RT}$$

by plotting ln q versus 1/T at constant conversion. The preexponential factor, k_0, can be determined knowing f(c), that means conversion and kinetics have to be known. These data permit then a computer simulation of a reactor runaway scenario. Keller et al. (1997) employed a series of chemical kinetic models to simulate the DSC experimental technique suitable for preliminary safety assessment and as an aid to preliminary screening (see simulation example DSC).

3.2.10
Process Development in the Fine Chemical Industry

As many other industries, the fine chemical industry is characterized by strong pressures to decrease the time-to-market. New methods for the early screening of chemical reaction kinetics are needed (Heinzle and Hungerbühler, 1997). Based on the data elaborated, the digital simulation of the chemical reactors is possible. The design of optimal feeding profiles to maximize predefined profit functions and the related assessment of critical reactor behavior is thus possible, as seen in the simulation examples RUN and SELCONT.

3.2.11 Chemical Reactor Waste Minimisation

The optimal design and operation of chemical reactors lies at the highest point of the waste minimisation hierarchy, in facilitating a reduction in the production of waste directly at source though eventually the behaviour of a production process as a whole is decisive (Heinzle et al., 2006). Ullmann's Encyclopedia (1995) describes many significant industrial process improvements that have resulted from direct waste reduction at source initiatives. These include the development of new process routes, equilibrium shifts to improve productivities, improvements in selectivity, new catalyst developments, process optimisation changes, reaction material changes, raw material purity changes, the employment of less harmful process materials and improved recycle and reuse of waste residues. In carrying out such new process initiatives, the combination of chemical reactor design theory and process chemistry is one that provides considerable opportunities for the exercise of flair and imagination. The chemical reactor is now recognised as the single most important key item in the chemical process and especially in regard to waste minimisation, where the emphasis is being applied increasingly to the maximum utilisation of reactants, maximum production of useful products and minimisation of wasteful by-products. In this, it is important to choose the optimum process chemistry, the best chemical reaction conditions and the most appropriate form and mode of operation for the actual chemical reactor. The importance of the reactor, in this respect, lies in the dependence of chemical reaction rates on reactant concentration and temperature. Thus the manipulation of concentration and temperature levels within the reactor provides an opportunity to directly manipulate relative reaction rates and to force reactions towards higher degrees of conversion and towards higher selectivities for the desired products as compared to byproduct wastes.

The above principles have been recognised since the very beginnings of chemical reactor design theory and are well treated in conventional reactor design textbooks. The topic is also given special emphasis with respect to the minimisation of waste by Smith (1995). The importance of the very early consideration of waste minimisation in an integrated process development strategy has also been highlighted by Heinzle and Hungerbühler (1997). In this latter respect, digital simulation forms a very important adjunct in enabling a detailed study of many prospective alternatives at the earliest design stage. An essential part of this process is the application of modelling and simulation techniques, particularly using models that are formulated as simply as possible with minimum complexity; a topic stressed extensively throughout this book. Important aspects of waste minimisation, as allied to chemical reactor design and operation, are illustrated in many of the accompanying digital simulation examples as follows: BATSEQ involving optimum reaction time; BATCOM, HYDROL, RELUY, BENZHYD, ANHYD, REVREACT and REVTEMP having optimal temperature or optimum temperature profiling strategies; CASCSEQ, SEMIPAR and SEMISEQ with optimal feed distribution policies; REXT featuring increased

conversion via in situ product removal and BATSEQ, SEMISEQ and COMPSEQ describing feed segregation effects.

In all these examples, the relevant waste minimisation aspects can be usefully studied simply in terms of the relative distribution of reaction compounds produced or by an extension of the programs to include possible quantification. A useful method of comparison is the "environmental index" as defined by Sheldon (1994), as the mass ratio of the total waste to that of useful product He showed that this index is very dependent both on the scale and chemical complexity of the process, with values ranging from about 0.1 for oil refining applications, up to 50 for fine chemical production and up to 100 plus for pharmaceutical operations. It thus reflects both the smaller scale of production, the greater usage of batch and semi batch operations and the greater complexity of the chemical processes. Sheldon also suggested the use of an environmental quotient, defined as $E_Q = E\ Q$, where Q is an arbitrary quotient related to the degree of environmental damage, with Q varying from 1 for simple compounds and up to 1000 for very destructive compounds.

Heinzle et al. (1998), Koller et al. (1998), Biwer and Heinzle (2004) and Heinzle et al. (2007) have described a simple but slightly more elaborate methodology to calculate such an environmental quotient based on more detailed material balances. Alternatively in terms of the present simulation examples, the analysis may perhaps be extended simply by means of incorporating a simple weighting or cost factor for each material to account for positive sales value or negative cost values representing the potential damage to the environment, as suggested in simulation example BATSEQ. A full analysis of any reactor or process simulation must of course take full account of all the relevent aspects, and Heinzle et al. (1998) and Koller et al. (1998) describe detailed studies as to how this might best be achieved.

Simulation Considerations

The waste minimisation reaction related examples in this text are represented mainly by combinations of consecutive and parallel type reactions. Although the major details of such problems are dealt with in conventional textbooks, it may be useful to consider the main aspects of such problems from the viewpoint of solution by digital simulation.

Consider the following first order consecutive reaction sequence

$$A \xrightarrow{k_1} B \xrightarrow{k_2} C$$

Solving the kinetic equations clearly demonstrates that the concentration of B passes through a maximum in respect to reaction time. If B is the desired product and C is waste, an optimal time t_{opt} can be defined for the maximum concentration of B, and where both the optimal yield and optimum reaction time

are functions of the kinetic rate constants k_1 and k_2. In waste minimisation terms, however, the quantity of B obtained both in relation to the unreacted A and waste product C is important, since these may represent quite distinct separation problems and may also have quite distinct associated environmental loadings. In general, one wants the rate of decomposition of A to B to be high relative to the rate of decomposition of B to C. Since these rates are also temperature dependent, a favourable product distribution can also be effected by varying the reaction temperature.

Now consider the following parallel reaction where A and B are reactants, P is useful product and Q is by-product waste.

$$A + B \xrightarrow{k_1} P$$

$$A + B \xrightarrow{k_2} Q$$

It is obviously important to achieve complete reaction for A and B and high selectivity for the formation of P with respect to Q.

The individual rates of reaction may be given by

$$r_P = k_1 C_A^{nA1} C_B^{nB1}$$

and

$$r_Q = k_2 C_A^{nA2} C_B^{nB2}$$

where n_{A1} and n_{A2} and n_{B1} and n_{B2} are the respective reaction for reactions 1 and 2.

The relative selectivity for the reaction is given by

$$\frac{r_P}{r_Q} = \frac{k_1}{k_2} C_A^{(nA1-nA2)} C_B^{(nB1-nB2)}$$

Thus if $n_{A1} > n_{A2}$, high selectivity for P is favoured by maintaining the concentration of A high. Conversely if $n_{A1} < n_{A2}$, high selectivity is favoured by low concentration of B.

With the orders of reaction being equal in both reactions

$$\frac{r_P}{r_Q} = \frac{k_1}{k_2}$$

where k_1 and k_2 are both functions of temperature, again showing that a favourable selectivity can be obtained by appropriate adjustment of the reactor temperature.

These and other waste minimisation considerations can be explored more fully both by reference to conventional texts and by simulation.

3.2.12 Non-Ideal Flow

The previous analysis of stirred-tank reactors has all been expressed in terms of the idealised concept of perfect mixing. In actual reactors, the mixing may be far from perfect and for continuous flow reactors may lie somewhere between the two idealised instances of perfect mixing and perfect plug flow, and may even include dead zones or short-cut flow. The concept of ideal plug flow is usually considered in terms of continuous tubular or continuous column type devices and the application of this to continuous flow reactors is discussed in Section 4.3.1. In ideal plug-flow reactors, all elements of fluid spend an identical period of time within the reactor, thus giving a zero distribution of residence times. All elements of fluid thus undergo an equal extent of reaction, and temperatures, concentrations and fluid velocities are completely uniform across any flow cross section. For a well-mixed, continuous stirred-tank reactor, however, there will be elements of fluid with, theoretically, a whole range of residence times varying from zero to infinity. Practical reactors will normally exhibit a distribution of residence times, which lie somewhere between these two extreme conditions and which effectively determine the performance of the reactor. The form of the residence time distribution curve can therefore be used to characterise the nature of the flow in the reactor, and models of the mixing behaviour can be important in simulations of reactor performance. Often different combinations of tanks in series or in parallel can be used to represent combinations of differing mixed flow regions and provide a powerful tool in the analysis of actual reactor behaviour.

Using Tracer Information in Reactor Design

Residence time distributions can be determined in practice by injecting a non-reactive tracer material into the input flow to the reactor and measuring the output response characteristics in a similar manner to that described previously in Section 2.1.1.

Unfortunately RTD studies cannot distinguish between early mixing and late mixing sequences of different types. Whereas the mixing history does not influence a first-order reaction, other reaction types are affected; the more complex the reaction kinetics the more the reaction selectivity or product distribution generally will be influenced. Thus for certain kinetic cases a detailed knowledge of the mixing can be important to the reactor performance. In practice this information may be difficult to obtain. In principle, tracer injection and sampling at different points in the reactor can supply the needed information. In practice, the usual procedure is to develop a model based on RTD experiments and the modeller's intuition. A comparison of the actual reactor performance with the

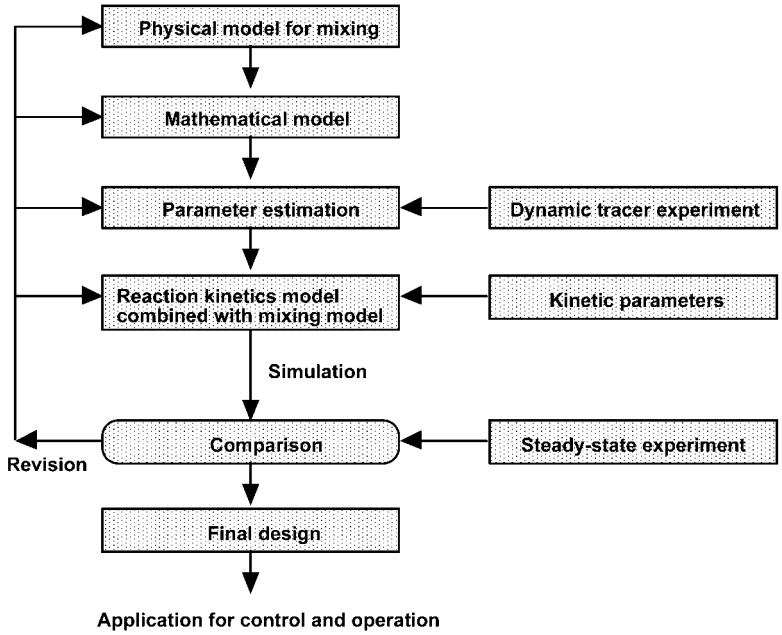

Fig. 3.20 Reactor design procedure with reactors having residence time distributions deviating from those of ideal reactors.

model predictions for known reaction kinetics reveals then whether the model assumptions were correct. The procedure is outlined above in Fig. 3.20.

Simulation examples demonstrating non-ideal mixing phenomenon in tank reactors are CSTRPULSE, NOCSTR and TUBEMIX. Other more general examples demonstrating rank-based residence time distributions are MIXFLO1, MIXFLO2, GASLIQ1, GASLIQ2 and SPBEDRTD.

3.2.13 Tank-Type Biological Reactors

Fermentation systems obey the same fundamental mass and energy balance relationships as do chemical reaction systems, but special difficulties arise in biological reactor modelling, owing to uncertainties in the kinetic rate expression and the reaction stoichiometry. In what follows, material balance equations are derived for the total mass, the mass of substrate and the cell mass for the case of the stirred tank bioreactor system (Dunn et al., 2003).

As indicated below in Fig. 3.21, feed enters the reactor at a volumetric flow rate F_0, with cell concentration X_0 and substrate concentration S_0. The vessel contents, which are well-mixed, are defined by volume V, substrate concentration S_1 and cell concentration X_1. These concentrations are identical to those of the outlet stream, which has a volumetric flow rate F_1.

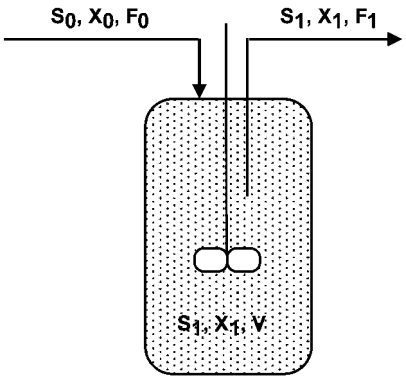

Fig. 3.21 Tank fermenter variables.

As shown previously, the general balance form can be derived by setting:

(Rate of accumulation) = (Input rate) − (Output rate) + (Production rate)

and can be applied to the whole volume of the tank contents.

Expressing the balance in equation form gives:

Total mass balance: $$\frac{d(V\rho)}{dt} = \rho(F_0 - F_1)$$

Substrate balance: $$\frac{d(VS_1)}{dt} = F_0S_0 - F_1S_1 + r_SV$$

Organism balance: $$\frac{d(VX_1)}{dt} = F_0X_0 - F_1X_1 + r_XV$$

where the units are: V (m^3), ρ (kg/m^3), F (m^3/s), S (kg/m^3), X (kg/m^3) with r_S and r_X (kg/m^3 s).

The rate expressions can be simply given by the Monod Equation:

$$r_X = \mu X_1$$

and

$$\mu = \frac{\mu_m S_1}{K_S + S_1}$$

using a constant yield coefficient

$$r_S = \frac{r_X}{Y_{X/S}}$$

but other forms of rate equation may equally apply.

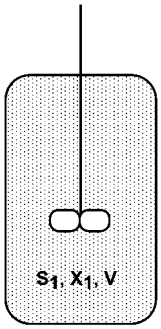

Fig. 3.22 The batch fermenter and variables.

The above generalised forms of equations can be simplified to fit particular cases of bioreactor operation.

3.2.13.1 **The Batch Fermenter**

Starting from an inoculum (X at t=0) and an initial quantity of limiting substrate, S at t=0, the biomass will grow, perhaps after a short lag phase, and will consume substrate. As the substrate becomes exhausted, the growth rate will slow and become zero when substrate is completely depleted. The above general balances can be applied to describe the particular case of a batch fermentation (constant volume and zero feed). Thus,

Total balance: $$\frac{dV}{dt} = 0$$

Substrate balance: $$V\frac{dS_1}{dt} = r_S V$$

Organism balance: $$V\frac{dX_1}{dt} = r_X V$$

Suitable rate expressions for r_S and r_X and the specification of the initial conditions would complete the batch fermenter model, which describes the exponential and limiting growth phases but not the lag phase.

3.2.13.2 **The Chemostat**

The term chemostat refers to a tank fermentation which is operated continuously. This bioreactor mode of operation normally involves sterile feed ($X_0=0$), constant volume and steady state conditions, meaning that $dV/dt=0$, $d(VS_1)/dt=0$, $d(VX_1)/dt=0$.

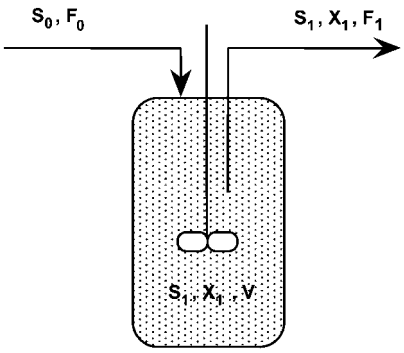

Fig. 3.23 The chemostat and its variables.

For constant density the total mass balance simplifies to

$$0 = F_0 - F_1$$

which means that the flow rates in and out of the bioreactor must be equal.

The dynamic component balance equations are then

Substrate balance: $$V\frac{dS_1}{dt} = F(S_0 - S_1) + r_S V$$

Cell balance: $$V\frac{dX_1}{dt} = -FX_1 + r_X V$$

where F is the volumetric flow through the system.

At steady state, $dS_1/dt=0$ and $dX_1/dt=0$.

Hence for the substrate balance:

$$0 = F(S_0 - S_1) + r_S V$$

and for the cell balance:

$$0 = -FX_1 + r_X V$$

Inserting the Monod-type rate expressions gives:

For the cell balance

$$\frac{FX_1}{V} = r_X = \mu X_1$$

or simply

$$\mu = \frac{F}{V} = D$$

Here D is the dilution rate and is equal to $1/\tau$, where τ = V/F and is equal to the mean residence time of the tank.

For the substrate balance:

$$F(S_0 - S_1) = \frac{r_X}{Y_{X/S}} V$$

from which

$$X_1 = Y_{X/S}(S_0 - S_1)$$

Thus, the specific growth rate in a chemostat is controlled by the feed flow rate, since μ is equal to D at steady state conditions. Since μ, the specific growth rate, is a function of the substrate concentration, and since μ is also determined by dilution rate, then the flow rate F also determines the outlet substrate concentration S_1. The last equation is, of course, simply a statement that the quantity of cells produced is proportional to the quantity of substrate consumed, as related by the yield factor $Y_{X/S}$.

If the flow rate F is increased, D will also increase, which causes the steady state value of S_1 to increase and the corresponding value of X_1 to decrease. It can be seen by simulation that when D nears μ_m, X_1 will become zero and S_1 will rise to the inlet feed value S_0. This corresponds to a complete removal of the cells by flow out of the tank, and this phenomenon is known as "washout".

3.2.13.3 **The Feed Batch Fermenter**

This bioreactor mode refers to a tank fermenter operated semi-continuously. The rate of the feed flow, F_0, may be variable, and there is no outlet flow rate from the fermentor. As a consequence of feeding the reactor volume will change with respect to time.

The balance equations then become for constant density

$$\frac{dV}{dt} = F_0$$

$$\frac{d(VS_1)}{dt} = F_0 S_0 + r_S V$$

$$\frac{d(VX_1)}{dt} = r_X V$$

Here the quantities VS_1 and VX_1 represent the masses of substrate and biomass, respectively, in the reactor. In a simulation, dividing these masses by the volume V gives the concentrations S_1 and X_1 as a function of time and which are needed in the appropriate kinetic relationships to calculate r_S and r_X.

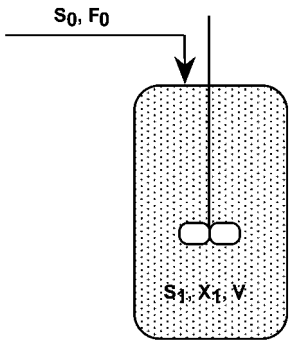

Fig. 3.24 Fed batch fermenter variables.

It can be shown by simulation that a quasi-steady state can be reached for a fed-batch fermenter, where $dX_1/dt = 0$ and $\mu = F/V$ (Dunn and Mor, 1975). Since V increases, μ must therefore decrease, and thus the reactor moves through a series of changing steady states for which $\mu = D$, during which S_1 and μ decrease, and X_1 remains constant. A detailed analysis of fed batch operation has been made by Keller and Dunn (1978).

All three bioreactor modes described above can be simulated using the example BIOREACT.

3.3 Stagewise Mass Transfer

3.3.1 Liquid-Liquid Extraction

Liquid-liquid extraction is an important chemical engineering separation process, and a knowledge of the process dynamics is important since many solvent extraction operations are still carried out batchwise. In addition, although most continuous solvent extraction plants are still designed on a steady-state basis, there is an increasing awareness of the need to assess possible safety and environmental risks at the earliest possible design stage. For this, a knowledge of the probable dynamic behaviour of the process becomes increasingly important. This applies, especially, in the fields of nuclear reprocessing and heavy metal extraction.

The modelling of solvent extraction is also of interest, since the dynamic behaviour of both liquid phases can be important, and because of the wide range of equipment types that can be employed and the wide range of dynamic behaviour that results. The equipment is typified by mixer–settlers at one extreme, often representing high capacity, stagewise contacting devices, in which near equilibrium conditions are achieved with slow, stable, but long-lasting dynamic char-

acteristics. At the other extreme are differential column devices, representing high throughput, low volume, non-equilibrium, differential contacting devices, with fast-acting dynamic behaviour. These columns have a limited range of permissible operating conditions and often an inherent lack of stability, especially when plant conditions are changing rapidly. Truly differential column devices are considered in Chapter 4, but some types of extraction columns can be regarded basically as stagewise in character, since the modelling of the dynamic characteristics of this type of device leads quite naturally from the equilibrium stagewise approach.

The treatment is confined to the use of two completely immiscible liquid phases, the feed or aqueous phase and the solvent or organic phase. No attempt is made to apply the modelling methodology to the case of partially miscible systems. Although one of the phases, the dispersed phase, will be in the form of droplets, dispersed in a continuum of the other, this is simplified by assuming each liquid phase to consist of separate well-mixed stage volumes. The modelling approach, shown in this chapter, follows the general modelling methodology in that it starts with the simplest case of a single component, batch extraction and then builds in further complexities. Finally a complex model of a non-ideal flow in a multistage, multicomponent, extraction cascade, which includes a consideration of both hydrodynamic effects and control, is achieved.

3.3.1.1 **Single Batch Extraction**

Volumes V_L and V_G of the two immiscible liquid phases are added to the extraction vessel and a single solute distributes itself between the phases as concentrations X and Y, respectively, at a rate, Q, as shown in Fig. 3.25.

For batch extraction, with no feed into the system, the component balances on each phase are given by:

$$\begin{pmatrix}\text{Rate of accumulation}\\ \text{of solute in}\\ \text{the given phase}\end{pmatrix} = \pm \begin{pmatrix}\text{Effective rate of}\\ \text{mass transfer to}\\ \text{or from the phase}\end{pmatrix}$$

Neglecting the effects of concentration changes on solvent density, the phase volumes will remain constant. Thus for the liquid phase with volume V_L

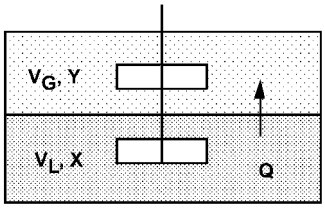

Fig. 3.25 Single-solute batch extraction between immiscible liquid phases.

$$V_L \frac{dX}{dt} = -Q$$

and for liquid phase with volume V_G

$$V_G \frac{dY}{dt} = +Q$$

where Q is the rate of solute transfer with units (mol/s) or (kg/s)

$$Q = K_L a(X - X^*)V$$

K_L is the mass transfer coefficient for the L phase (m/s), a is the interfacial area per unit volume (m^2/m^3), referred to the total liquid volume of the extractor, V is the total holdup volume of the tank, and is equal to ($V_L + V_G$). X^* is the equilibrium concentration, corresponding to concentration Y, given by

$$X^* = f_{eq}(Y)$$

as illustrated in Fig. 3.26.

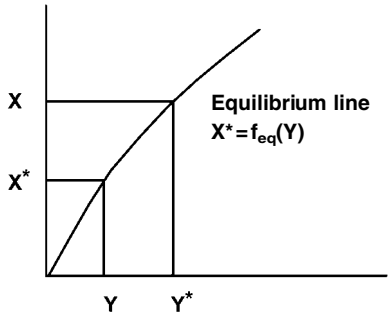

Fig. 3.26 Equilibrium relationship between two liquid phases.

The information flow diagram (Fig. 3.27) for this system shows the two component material balance relations to be linked by the equilibrium and transfer rate relationships.

Note that the transfer rate equation is based on an overall concentration driving force ($X - X^*$) and overall mass transfer coefficient K_L. The two-film theory for interfacial mass transfer shows that the overall mass transfer coefficient, K_L, based on the L-phase is related to the individual film coefficients for the L and G-phase films, k_L and k_G, by the relationship

$$\frac{1}{K_L} = \frac{1}{k_L} + \frac{m}{k_G}$$

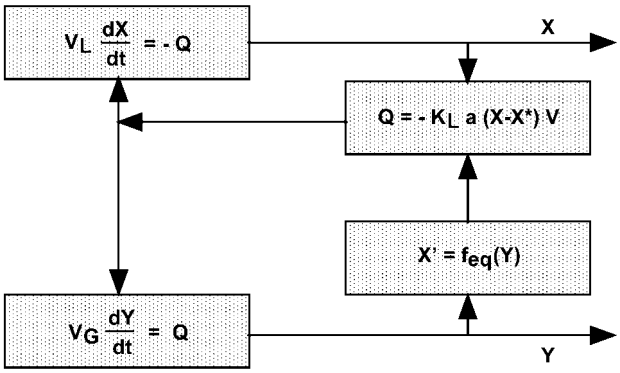

Fig. 3.27 Information flow diagram for simple batch extraction.

where m is the slope of the equilibrium curve and

$$\frac{dY^*}{dX} = m$$

For a linear equilibrium curve with constant film coefficients, k_L and k_G, the overall coefficient, K_L, will also be constant, but for the case of a non-linear equilibrium relationship, the value of m, which is the local slope of the equilibrium curve, will vary with solute concentration. The result is that the overall coefficient, K_L, will also vary with concentration, and therefore in modelling the case of a non-linear equilibrium extraction, further functional relationships relating the mass transfer coefficient to concentration will be required, such that

$$K_L = f(X)$$

3.3.1.2 **Multisolute Batch Extraction**

Two solutes distribute themselves between the two phases as concentrations X_A and Y_A, and X_B and Y_B and with rates Q_A and Q_B, respectively, as shown in Fig. 3.28. The corresponding equilibrium concentrations X_A^* and X_B^* are functions of both the interacting solute concentrations, Y_A and Y_B, and can be expressed by functional relationships of the form

$$X_A^* = f_{Aeq}(Y_A, Y_B)$$

$$X_B^* = f_{Beq}(Y_A, Y_B)$$

Typical representations of the way that the two differing equilibrium relationships can interact are shown in Fig. 3.29, and it is assumed that the equilibria can be correlated by appropriate, explicit equation forms.

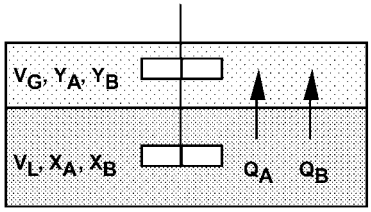

Fig. 3.28 Two-solute batch extraction.

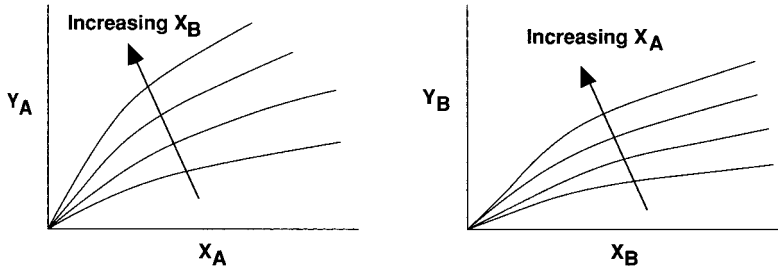

Fig. 3.29 Interacting solute equilibria for the two solutes A and B.

For multi-component systems, it is necessary to write the dynamic equation for each phase and for each solute, in turn. Thus, for phase volume V_L, the balances for solute A and for solute B are

$$V_G \frac{dY_A}{dt} = K_{LA} a (X_A - X_A^*) V_L$$

$$V_G \frac{dY_B}{dt} = K_{LB} a (X_B - X_B^*) V_L$$

The overall mass transfer coefficients are also likely to vary with concentration, owing to the complex multisolute equilibria, such that

$$K_{LA} = f_A(X_A, X_B)$$

$$K_{LB} = f_B(X_A, X_B)$$

Again, these functional relationships should ideally be available in an explicit form in order to ease the numerical method of solution. Two-solute batch extraction is covered in the simulation example TWOEX.

3.3.1.3 **Continuous Equilibrium Stage Extraction**

Here the extraction is carried out continuously in a single, perfectly mixed, extraction stage as shown in Fig. 3.30. It is assumed that the outlet flow concen-

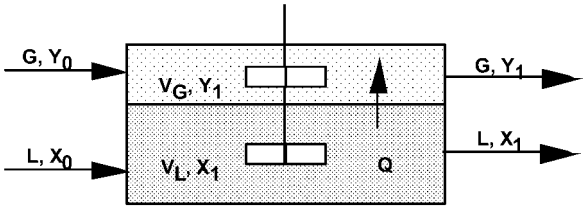

Fig. 3.30 Continuous equilibrium stage extraction.

trations, X_1 and Y_1, achieve equilibrium and that density variations are negligible.

Following an initial transient, the extractor will achieve a steady state operating condition, in which the outlet concentrations remain constant with respect to time.

At steady state, the quantity of solute entering the extractor is equal to the quantity of solute leaving. A steady-state balance for the combined two-phase system gives

$$LX_0 + GY_0 = LX_1 + GY_1$$

where for an equilibrium stage extraction

$$X_1 = f_{eq}(Y_1)$$

Here, L and G are the volumetric flow rates of the heavy and the light phases, respectively, X_0 and Y_0 are the respective inlet solute concentrations of the two phases, X_1 and Y_1 are the respective outlet solute concentrations.

For a linear equilibrium relationship

$$Y_1 = mX_1$$

A simple substitution of the value Y_1 in the balance equation enables the steady-state concentration X_1 to be determined, where

$$X_1 = \frac{(LX_0 + GY_0)}{(L + mG)}$$

The steady-state approach, however, provides no information on the initial transient conditions, whereby the extractor achieves eventual steady state or on its dynamic response to disturbances.

The eventual steady state solution may often be also very difficult to calculate for cases in which the equilibrium is non-linear or where complex interacting equilibria for multicomponent mixtures are involved. In such instances, we have found a dynamic solution to provide a very simple means of solution.

The dynamic component balance equations for each of the two phases in turn.

$$\begin{pmatrix}\text{Rate of}\\ \text{accumulation}\\ \text{of solute}\end{pmatrix} = \begin{pmatrix}\text{Rate of}\\ \text{flow in}\\ \text{of solute}\end{pmatrix} - \begin{pmatrix}\text{Rate of}\\ \text{flow out}\\ \text{of solute}\end{pmatrix} \pm \begin{pmatrix}\text{Rate}\\ \text{of solute}\\ \text{transfer}\end{pmatrix}$$

The sign of the transfer term will depend on the direction of mass transfer. Assuming solute transfer again to proceed in the direction from volume V_L to volume V_G, the component material balance equations become for volume V_L

$$V_L \frac{dX_1}{dt} = LX_0 - LX_1 - Q$$

and for volume V_G

$$V_G \frac{dY_1}{dt} = GY_0 - GY_1 + Q$$

where

$$Q = K_L a(X_1 - X_1^*)V_L$$

For an equilibrium stage, the outlet concentrations leaving the stage are in equilibrium, i.e.

$$X_1^* = f_{eq}(Y_1)$$

Here an arbitrarily high value for the mass transfer coefficient K_L can be used to force a close approach to equilibrium. Thus for a finite value of the rate of transfer Q, the driving force will be very small, and hence the value of X_n^* is forced to be very close to X_n. The final near equilibrium condition is thus achieved as a result of the natural cause and effect in which equilibrium is favoured by a high mass transfer coefficient, which is used here simply as a high gain forcing factor, in the manner originally suggested by Franks (1972). Using this technique, some additional problems in solution may be experienced due to stiffness caused by a too high value for K_L, but using the fast numerical integration routines of MADONNA, such difficulties become rather minimal.

This dynamic approach to equilibrium method is used in later examples to illustrate its further application to the solution of complex steady state problems.

Continuous single-stage extraction is treated in the simulation example EQEX. Chemical reaction with integrated single stage extraction is demonstrated in the simulation example REXT.

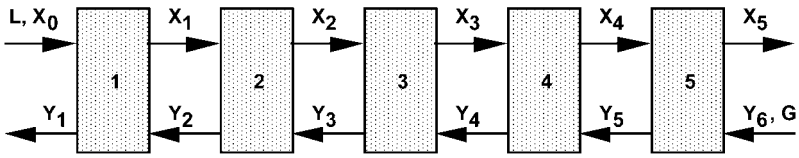

Fig. 3.31 Multistage countercurrent extraction cascade.

3.3.1.4 **Multistage Countercurrent Extraction Cascade**

For a high degree of extraction efficiency, it is usual to connect several continuous flow stages to form a countercurrent flow extraction cascade, as indicated in Fig. 3.31.

In each stage, it is assumed that the two phases occupy well-mixed, constant volumes V_L and V_G. The phase volumes V_L and V_G can, however, vary from stage to stage along the cascade. This effect is easily included into any simulation program. Additional complexity, in the formulation of the model, is now provided by the requirement of having to write balance equations for each of the stages of the cascade. The total number of equations to be solved is thus increased, but the modelling procedure remains straightforward.

For any given stage, n, the component material balance equations for each phase are thus defined by

$$V_{Ln}\frac{dX_n}{dt} = L(X_{n-1} - X_n) - Q_n$$

$$V_{Gn}\frac{dY_n}{dt} = G(Y_{n+1} - Y_n) + Q_n$$

where

$$Q_n = K_{Ln}A_n(X_n - X_n^*)V_n$$

and

$$X_n^* = f_{eq}(Y_n)$$

as shown in Fig. 3.32.

Note that the rate of transfer is defined by the local concentrations X_n and X_n^* appropriate to the particular stage, n. It is straightforward in the formulation of the model to allow for variations of the parameter values V_L, V_G, K_L and a from stage to stage and for both K_L and a to vary with respect to the local concentration. In order to do this, it is necessary to define new constant values for V_L and V_G for each stage and to have functional relationships, relating the mass transfer capacity coefficient to stage concentration. In order to model equilibrium stage behaviour, actual values of the mass transfer capacity product term (K_{Ln} a_n) would be again replaced by an arbitrary high value of the gain coefficient, K_{Ln}, to force actual stage concentrations close to the equilibrium. Multi-

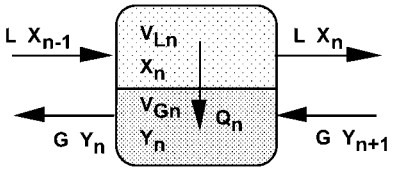

Fig. 3.32 Flow and composition inputs to stage n of the cascade.

stage extraction is treated in the simulation example EQMULTI, which permits calculation of the dynamics and steady state for situations in which the numbers of stages, flow rate and mass transfer conditions can all become variables in the simulation solution.

3.3.1.5 **Countercurrent Extraction Cascade with Backmixing**

The extension of the modelling approach to allow for backmixing between stages, cascades with side streams, or multiple feeds is also accomplished, relatively easily, by an appropriate modification of the inflow and outflow terms in the component balance equations (Ingham and Dunn, 1974). Backmixing reduces the efficiency of countercurrent mass transfer cascades, owing to its effect on the concentration profiles within the cascade and in decreasing the effective concentration driving forces. The effects of backmixing are especially severe in the case of solvent extraction columns. The stagewise model with backmixing is a well-known model representation, but the analytical solution is normally mathematically very complex and analytical solutions, both for steady-state and unsteady-state operating conditions, only apply for single-solute extraction where parameter values remain constant and furthermore where a linear equilibrium relationship applies. Compared to this, the solution of the dynamic model equations by digital simulation using MADONNA is far more general, since this has the ability to encompass varying parameter values, non-linear equilibria-multisolute systems plus a variable number of stages.

A multistage extraction cascade with backmixing is shown in Fig. 3.33. Here the backmixing flow rates L_B and G_B act in the reverse direction to the main phase flows, between the stages and along the cascade. One important factor in the modelling process is to realise that, as a consequence of the backmixing flows, since phase volumes remain constant, then the interstage flow rates along the cascade, in the forward direction, must also be increased by the magnitude of the appropriate backmixing flow contribution. With a backmixing flow L_B in the aqueous phase, the resultant forward flow along the cascade must now be $(L+L_B)$, since the backmixing does not appear exterior to the column. Similarly with a backmixed flow G_B, the forward flow for the organic phase is also increased to $(G+G_B)$. Taking into account the changed flow rates, however, the derivation of the component balance equations follows normal procedures.

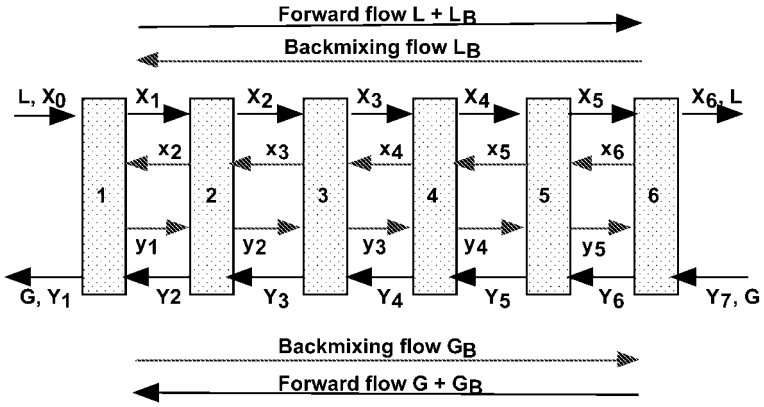

Fig. 3.33 Multistage extraction cascade with backmixing of both phases.

The relative inflow and outflow contributions for each phase of any stage n of the cascade is shown in Fig. 3.34.

Allowing for the additional backmixing flow contributions, the component balance equation for the two phases in stage n of the cascade are now

$$V_{Ln}\frac{dX_n}{dt} = (L + L_B)X_{n-1} - (L + L_B)X_n + L_B X_{n+1} - L_B X_n - Q_n$$

or

$$V_{Ln}\frac{dX_n}{dt} = (L + L_B)(X_{n-1} - X_n) + L_B(X_{n+1} - X_n) - Q_n$$

and

$$V_{Gn}\frac{dY_n}{dt} = (G + G_B)(Y_{n+1} - Y_n) + G_B(Y_{n-1} - Y_n) + Q_n$$

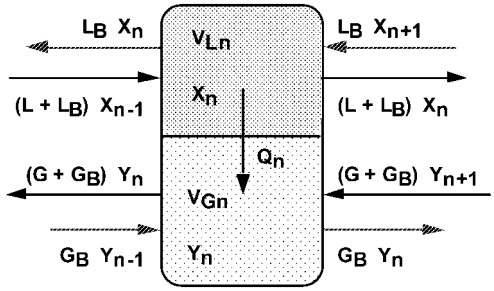

Fig. 3.34 Stage n of a multistage extraction cascade with backmixing.

Although more complex in form, the resulting model equations provide no major additional difficulty, and solution is also easily obtained. Multistage extraction with backmixing is covered in the simulation example EQBACK.

3.3.1.6 **Countercurrent Extraction Cascade with Slow Chemical Reaction**

A countercurrent extraction cascade with reaction $A + B \rightarrow C$ is shown in Fig. 3.35. The reaction takes place between a solute A in the L-phase, which is transferred to the G-phase by the process of mass transfer, where it then reacts with a second component, B, to form an inert product, C, such that A, B and C are all present in the G-phase.

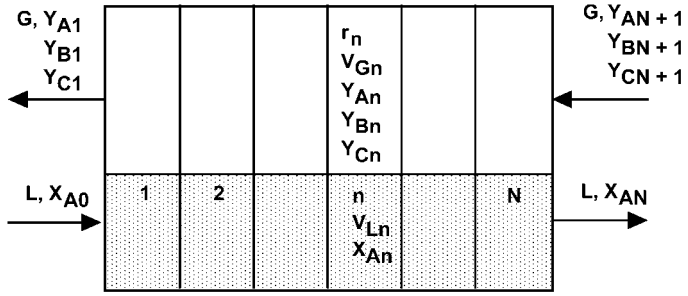

Fig. 3.35 Solute A is transferred from the L-phase to the G-phase, where it reacts with a component B, to form C.

The general component balance form of equation gives

$$\begin{pmatrix}\text{Rate of}\\ \text{accumulation}\\ \text{of solute}\\ \text{in phase i}\end{pmatrix} = \begin{pmatrix}\text{Inflow}\\ \text{rate of}\\ \text{solute}\\ \text{in phase i}\end{pmatrix} - \begin{pmatrix}\text{Outflow}\\ \text{rate of}\\ \text{solute}\\ \text{in phase i}\end{pmatrix} \pm \begin{pmatrix}\text{Rate of}\\ \text{solute}\\ \text{mass}\\ \text{transfer}\end{pmatrix} \pm \begin{pmatrix}\text{Rate of}\\ \text{solute}\\ \text{reaction}\end{pmatrix}$$

where for phase L

$$V_{Ln}\frac{dX_{An}}{dt} = L(X_{An-1} - X_{An}) - Q_{An}$$

and for phase G

$$V_{Gn}\frac{dY_{An}}{dt} = G(Y_{An+1} - Y_{An}) + Q_{An} - r_n V_{Gn}$$

Components B and C are both immiscible in phase L and remain in phase G. Therefore

$$V_{Gn}\frac{dY_{Bn}}{dt} = G(Y_{Bn+1} - Y_{Bn}) - r_n V_{Gn}$$

$$V_{Gn}\frac{dY_{Cn}}{dt} = G(Y_{Cn+1} - Y_{Cn}) + r_n V_{Gn}$$

where the transfer rate is

$$Q_{An} = K_{ALn}a_n(X_{An} - X^*_{An})V_n$$

and the reaction rate is

$$r_n = kY_{An}Y_{Bn}$$

Figure 3.36 shows the graphical output in the G-phase concentrations of component A with respect to time, starting the cascade at time t=0 with initially zero concentrations throughout. The maximum in the Y_{A1} profile for stage 1 is due to a delay of reactant B in reaching A. This is because A and B are fed from the opposite ends of the cascade, and thus a certain time of passage through the extractor is required before B is able to react with A in stage 1.

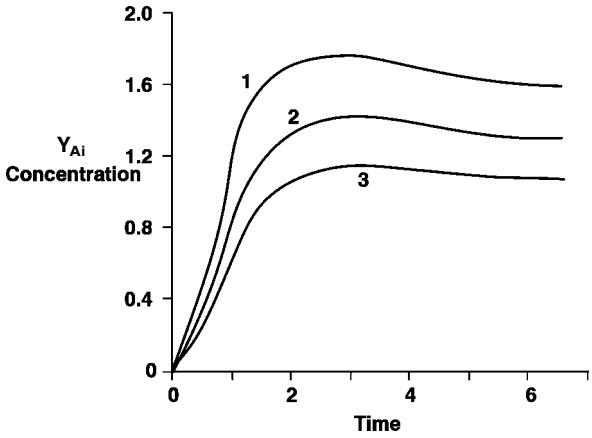

Fig. 3.36 Concentrations in the solvent phases of stages 1, 2 and 3 in a countercurrent extraction column with slow chemical reaction.

3.3.1.7 **Multicomponent Systems**

Assuming the liquid phases remain immiscible, the modelling approach for multicomponent systems remains the same, except that it is now necessary to write additional component balance equations for each of the solutes present, as for the multistage extraction cascade with backmixing in Section 3.2.2. Thus for component j, the component balance equations become

$$V_{Ln}\frac{dX_j}{dt} = (L + L_B)(X_{jn-1} - X_{jn}) + L_B(X_{jn+1} - X_{jn}) - Q_{jn}$$

$$V_{Gn}\frac{dY_j}{dt} = (G + G_B)(Y_{jn+1} - Y_{jn}) + G_B(Y_{jn-1} - Y_{jn}) + Q_{jn}$$

where

$$Q_{jn} = K_{Ljn}a_n(X_{jn} - X^*_{jn})V_n$$

The additional number of differential equations and increased complexities of the equilibrium relationships may also be compounded by computational problems caused by widely differing magnitudes in the equilibrium constants for the various components. As discussed in Section 3.3.2, it is shown that this can lead to widely differing values in the equation time constants and hence to stiffness problems for the numerical solution.

3.3.1.8 Control of Extraction Cascades

A typical control problem might be the maintenance of a required raffinate outlet concentration, Y_N, with the controller action required to compensate the effect of variations in the feed concentration Y_0, as indicated in Fig. 3.37.

The proportional-integral control equation, as given in Section 2.3.2.2, is:

$$L = L_0 + K_p\varepsilon(t) + \frac{K_p}{\tau_I}\int_0^t \varepsilon(t)dt$$

where L is the manipulated variable, i.e., the solvent flow rate, L_0 is the base value for L, K_p is the proportional gain, τ_I is the integral action time and ε is the error between the actual concentration Y_N and the desired value Y_{set}. These relationships can be directly incorporated into a digital simulation program as shown in example EXTRACTCON. If required, it is also possible to include the

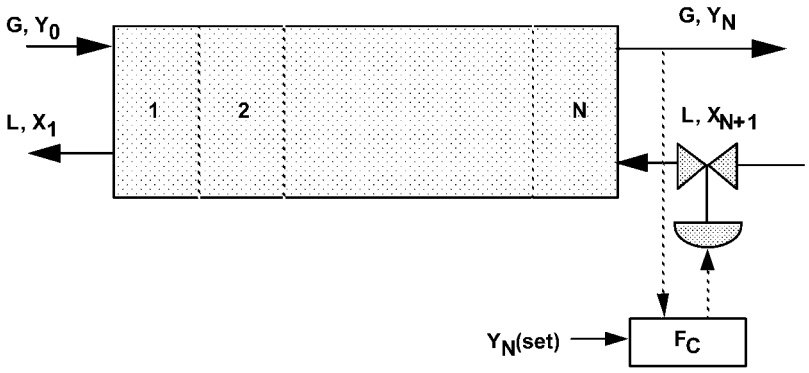

Fig. 3.37 Maintenance of raffinate outlet concentration, by regulation of solvent flow rate.

dynamic effects of the measuring elements, measurement transmitters, and the control valve characteristics into the simulation program as shown by Franks (1972) and Luyben (1990).

3.3.1.9 **Mixer–Settler Extraction Cascades**

The archetypal stagewise extraction device is the mixer–settler. This consists essentially of a well-mixed agitated vessel, in which the two liquid phases are mixed and brought into intimate contact to form a two-phase dispersion, which then flows into the settler for the mechanical separation of the two liquid phases by continuous decantation. The settler, in its most basic form, consists of a large empty tank, provided with weirs to allow the separated phases to discharge. The dispersion entering the settler from the mixer forms an emulsion band, from which the dispersed phase droplets coalesce into the two separate liquid phases. The mixer must adequately disperse the two phases, and the hydrodynamic conditions within the mixer are usually such that a close approach to equilibrium is obtained within the mixer. The settler therefore contributes little mass transfer function to the overall extraction device.

Ignoring the quite distinct functions and hydrodynamic conditions which exist in the actual mixer and settler items of the combined mixer–settler unit, it is possible, in principle, to treat the combined unit simply as a well-mixed equilibrium stage. This is done in exactly the way as considered previously in Sections 3.2.1 to 3.2.6. A schematic representation of an actual mixer–settler device is shown in Fig. 3.38 and an even more simplified representation of the equivalent simple well-mixed stage is given in Fig. 3.39.

A realistic description of the dynamic behaviour of an actual mixer–settler plant item should however also involve some consideration of the hydrodynamic characteristics of the separate mixer and settler compartments and the possible flow interactions between mixer and settler along the cascade.

The notation for separate mixer–settler units is shown in Fig. 3.40, for stage n of the cascade.

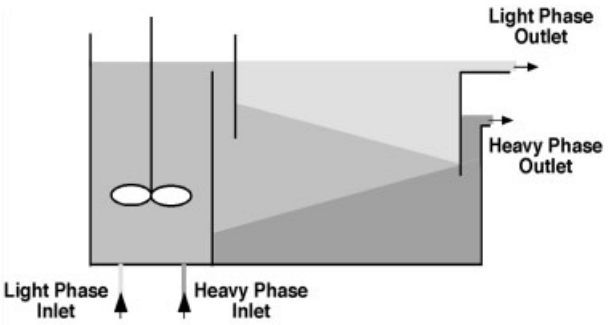

Fig. 3.38 Schematic representation of a mixer–settler unit.

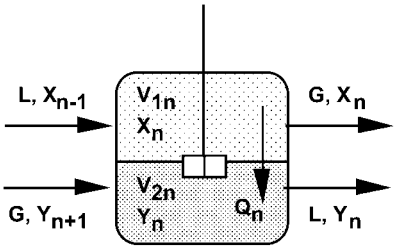

Fig. 3.39 The well-mixed stage representation of a mixer–settler unit.

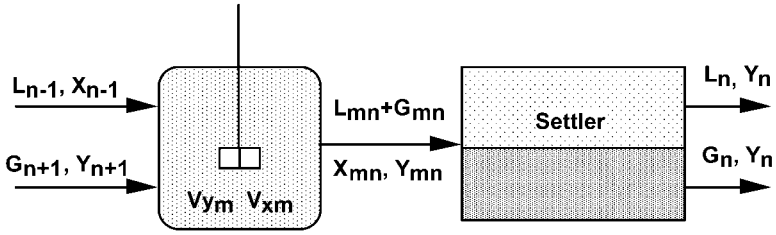

Fig. 3.40 The separate mixer and settler compartments for stage n of a mixer–settler cascade.

In this representation, the heavy phase with a flow rate, L_{n-1}, enters the mixer from the preceding stage n–1, together with solvent flow, G_{n+1}, from stage n+1. The corresponding phase flow rates, in the dispersion, leaving the mixer and entering the settler are shown as L_{mn} and G_{mn} and with concentrations X_{mn} and Y_{mn} respectively. This is to allow for possible changes in the volumetric holdup of the mixer following changes in flow rate. The modelling of the separate mixer and settler compartments follows that of Wilkinson and Ingham (1983).

Mixer Dynamics

Owing to the intensive agitation conditions and intimate phase dispersion, obtained within the mixing compartment, the mixer can usually be modelled as a single perfectly mixed stage in which the rate of mass transfer is sufficient to attain equilibrium. As derived previously in Section 3.3.1.3, the component balance equations for the mixer, based on the two combined liquid phases, is thus given by

$$\frac{d(V_{Lm}X_{mn} + V_{Gm}Y_{mn})}{dt} = L_{n-1}X_{n-1} + G_{n+1}Y_{n+1} - G_{mn}Y_{mn} - L_{mn}X_{mn}$$

where subscript m refers specifically to the conditions within the mixer and hence to the effluent flow, leaving the mixer and entering the settler.

The total material balance for the mixer is expressed by

$$\begin{pmatrix}\text{Rate of change of}\\ \text{mass in mixer}\end{pmatrix} = \begin{pmatrix}\text{Mass}\\ \text{flow in}\end{pmatrix} - \begin{pmatrix}\text{Mass}\\ \text{flow out}\end{pmatrix}$$

Neglecting the effects of any density changes, the total material balance then provides the relationship for the change of total volume in the mixer with respect to time.

$$\frac{d(V_{Lmn} + V_{Gmn})}{dt} = L_{n-1} + G_{n+1} - L_{mn} - G_{mn}$$

Under well-mixed flow conditions it is reasonable to assume that the mixer holdup volumes, V_{Lmn} and V_{Gmn}, will vary in direct proportion to the appropriate phase flow rate, and that the total liquid holdup in the mixer will vary as a function of the total flow rate to the mixer.

The total flow rate ($L_{mn}+G_{mn}$), leaving the mixer, will be related to the total phase volumes V_{Lm} and V_{Gm} by a hydrostatic equation, which will depend on the net difference in the head of liquid between the levels in the mixer and in the settler. The actual form of this relationship might need to be determined experimentally, but could, for example, follow a simple square-root relationship of the form in which flow rate is proportional to the square root of the difference in liquid head, or indeed to the total volume of liquid in the mixer, e.g.,

$$L_{mn} + G_{mn} \propto (V_{Lm} + V_{Gm})^{1/2}$$

The further assumptions are that the respective phase volumes are in direct proportion to the phase flow rate, i.e.,

$$\frac{V_{Lmn}}{V_{Gmn}} = \frac{L_{mn}}{G_{mn}}$$

and the concentrations leaving the mixer are in equilibrium according to

$$Y_{mn} = f_{eq}(X_{mn})$$

These equations complete a preliminary model for the mixer. Note that it is also possible, in principle, to incorporate changing density effects into the total material balance equation, provided additional data, relating liquid density to concentration, are available.

Settler Dynamics

The simplest settler model is that in which it is assumed that each phase flows through the settler in uniform plug flow, with no mixing and constant velocity. This has the effect that the concentrations leaving the settler, X_n and Y_n, are simply the time-delayed values of the exit mixer concentrations X_{mn} and Y_{mn}.

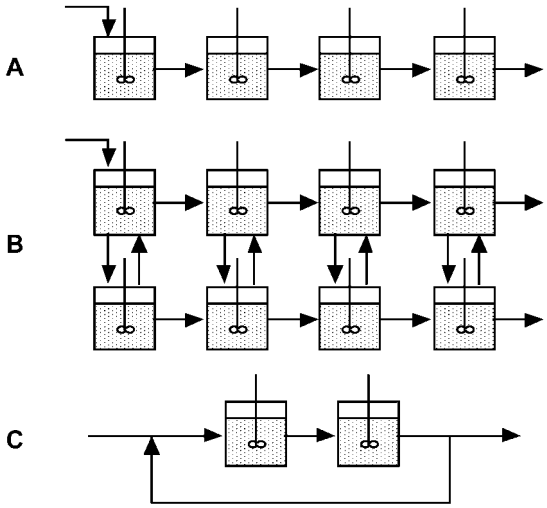

Fig. 3.41 Alternative settler-flow representations for the separate phases.

In this the magnitude of the time delay is thus simply the time required for the phase to pass through the appropriate settler volume.

The outlet phase flow rates, L_n and G_n, may again be related to the inlet settler phase flow rates, L_{mn} and G_{mn}, and settler phase volumes by hydraulic considerations, using similar formulations to those proposed for the mixer, as required.

In practice, some mixing will, however, occur in each phase of the settler, and various models involving either an arbitrary number of perfect mixing stages or various flow combinations, with and without recycle effects, can be postulated. Some of these are indicated in Fig. 3.41, where Fig. 3.41 A represents settler mixing, given by a series of stirred tanks, Fig. 3.41 B a series of well-mixed tanks interconnected to stagnant regions and Fig. 3.41 C a series of two tanks with recycle. The actual representation adopted for a given situation, would, of course, have to depend very much on the actual mechanical arrangement and flow characteristics of the particular settler design, together with actual observations of the flow behaviour.

Figure 3.42 shows one possible representation in which a proportion of each phase passes through the settler in plug flow, while the remaining proportion is well mixed.

The resultant outlet concentration from the settler is then given by the combined plug-flow and well-mixed flow streams.

The notation for the above flow model, in respect of the aqueous-phase settler volume, is shown in Fig. 3.43.

If L_{mn} is the volumetric flow rate of the heavy phase entering the settler from the mixer, and f is the fraction of flow passing through the plug-flow region with time delay t_{Dn}, then $L_{mn}f$ is the volumetric flow passing through the plug-

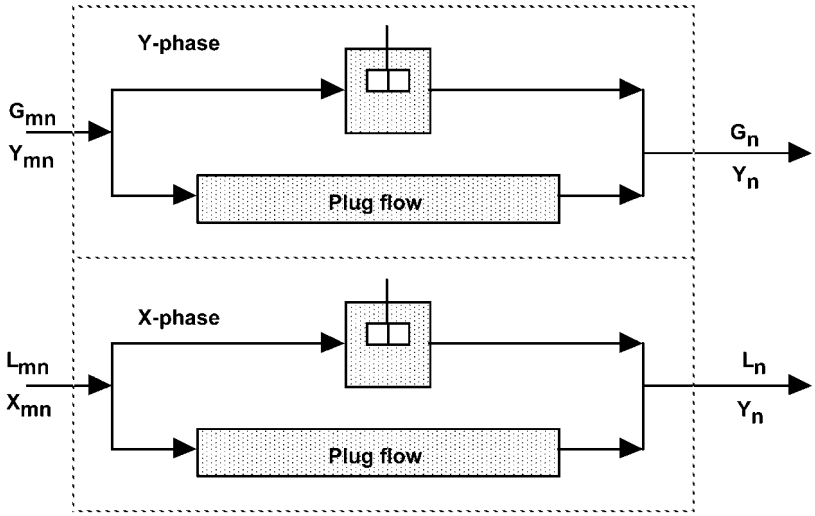

Fig. 3.42 Combined plug-flow and well-mixed settler-flow representation.

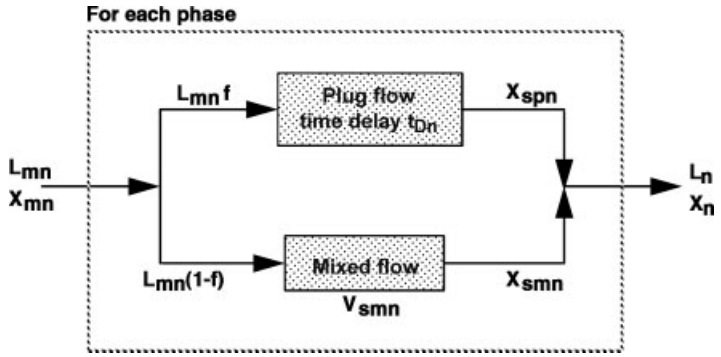

Fig. 3.43 Combined plug-flow and well-mixed flow representation for the heavy phase settler flow.

flow region. The concentration at the plug-flow region outlet, X_{spn}, is the inlet concentration at time $t-t_{Dn}$ and is given by

$$X_{spn} = X_{mn(t-t_{Dn})}$$

The fractional flow rate $L_{mn}(1-f)$ is then also the volumetric flow passing through the well-mixed region of settler phase volume, V_{mix}. The flows leaving the plug-flow and well-mixed regions X_{spn} and X_{smn}, respectively, then combine to give the actual exit concentration from the settler X_n.

The model equations for the heavy phase settler region then become for the well-mixed region

$$V_{smn}\frac{dX_{smn}}{dt} = L_{mn}(1-f)(X_{mn} - X_{smn})$$

and for the combined outlet phase flow

$$L_n X_n = L_{mn}(1-f)X_{smn} + L_{mn} f X_{spn}$$

Mixer–Settler Cascade

The individual mixer and settler model representations can then be combined into an actual countercurrent-low, multistage, extraction scheme representation as shown in Fig. 3.44. This includes an allowance for backmixing, between the stages of the cascade caused by inefficient phase disengagement in the settlers, such that a fraction f_L or f_G of the appropriate phase flow leaving the settler is entrained. This means it is actually carried back in the reverse direction along the cascade by entrainment in the other phase. It is assumed, for simplicity, that the total flows of each phase, L and G, remain constant throughout all the stages of the cascade. Entrainment fractions f_L and f_G are also assumed constant for all settlers. The above conditions, however, are not restrictive in terms of the capacity of the solution by digital simulation.

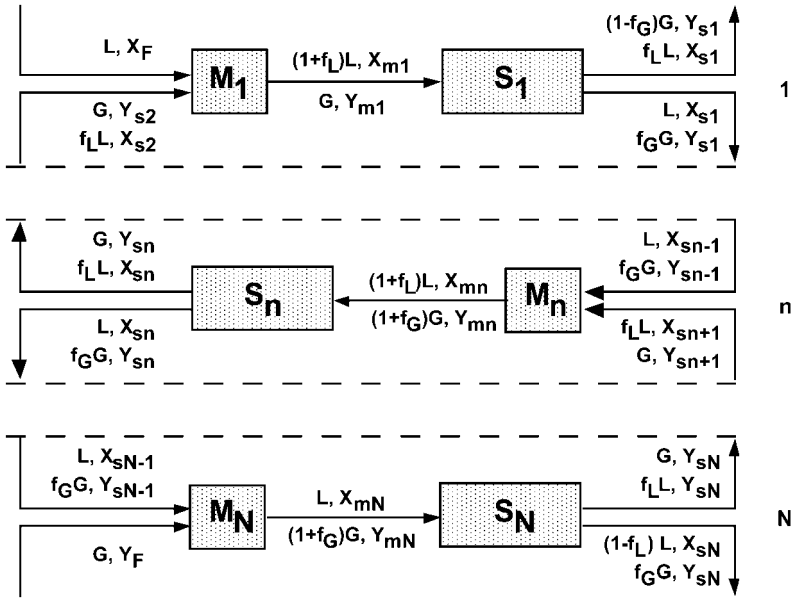

Fig. 3.44 Multistage mixer–settler cascade with entrainment backmixing. M and m refers to mixer and S and s to settler; stages are 1 to N.

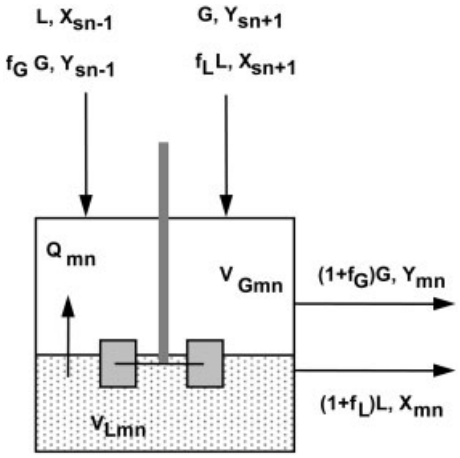

Fig. 3.45 One mixer–settler stage, n.

The conditions in the mixer of any stage n are represented in Fig. 3.45.

Allowing for the additional flow contributions due to the entrainment backmixing, the component balance equations, for any mixer n along the cascade, are now expressed by

$$V_{Lmn}\frac{dX_{mn}}{dt} = LX_{sn-1} + f_L LX_{sn+1} - (1+f_L)LX_{mn} - Q_{mn}$$

and

$$V_{Gmn}\frac{dY_{mn}}{dt} = GY_{sn+1} + f_G GY_{sn-1} - (1+f_G)GY_{mn} + Q_{mn}$$

where

$$Q_{mn} = K_L a_m (X_{mn} - X^*_{mn})V_{Lmn}$$

$$V_{mn} = V_{Lmn} + V_{Gmn}$$

The settler equations are as shown previously, but must, of course, be applied to both phases.

Figure 3.46 shows the output obtained from a full solution of the mixer–settler model. The effect of the time delay in the settlers, as the disturbance, as propagated through the system from stage to stage, is very evident.

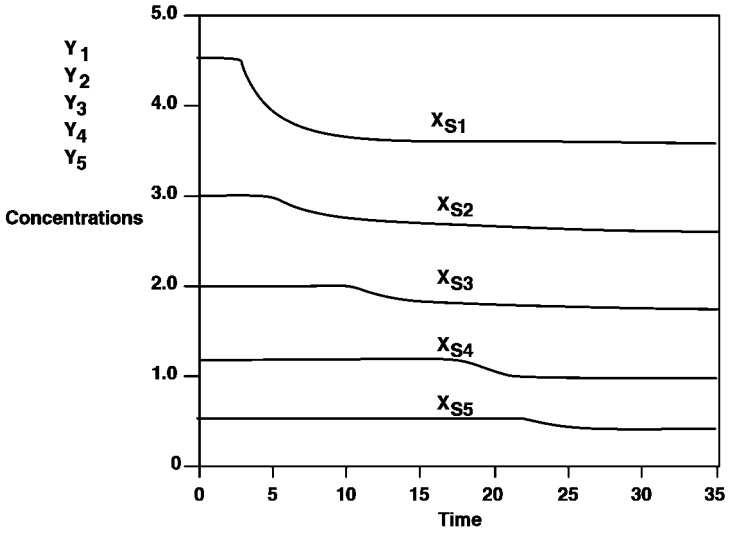

Fig. 3.46 Computer simulation output for a five-stage mixer–settler cascade with entrainment.

3.3.1.10 **Staged Extraction Columns**

A wide variety of extraction column forms are used in solvent extraction applications. Many of these, such as rotary-disc contactors (RDC), Oldshue–Rushton columns, and sieve-plate column extractors, have rather distinct compartments and a geometry which lends itself to an analysis of column performance in terms of a stagewise model. As the compositions of the phases do not come to equilibrium at any stage, however, the behaviour of the column is therefore basically differential in nature.

At the prevailing high levels of dispersion normally encountered in such types of extraction columns, the behaviour of these essentially differential type contactors, however, can be represented by the use of a non-equilibrium stagewise model.

The modelling approach to multistage countercurrent equilibrium extraction cascades, based on a mass transfer rate term as shown in Section 1.4, can therefore usefully be applied to such types of extractor column. The magnitude of the mass transfer capacity coefficient term, now used in the model equations, must however be a realistic value corresponding to the hydrodynamic conditions, actually existing within the column and, of course, will be substantially less than that leading to an equilibrium condition.

In Fig. 3.47 the column contactor is represented by a series of N non-equilibrium stages, each of which is of height H and volume V. The effective column height, Z, is thus given by $Z = N\,H$.

The stagewise model with backmixing is an essential component of any model representation of a stagewise extraction column. As shown in Section 3.3.1.5 the non-ideal flow behaviour is represented by the presence of the N stages

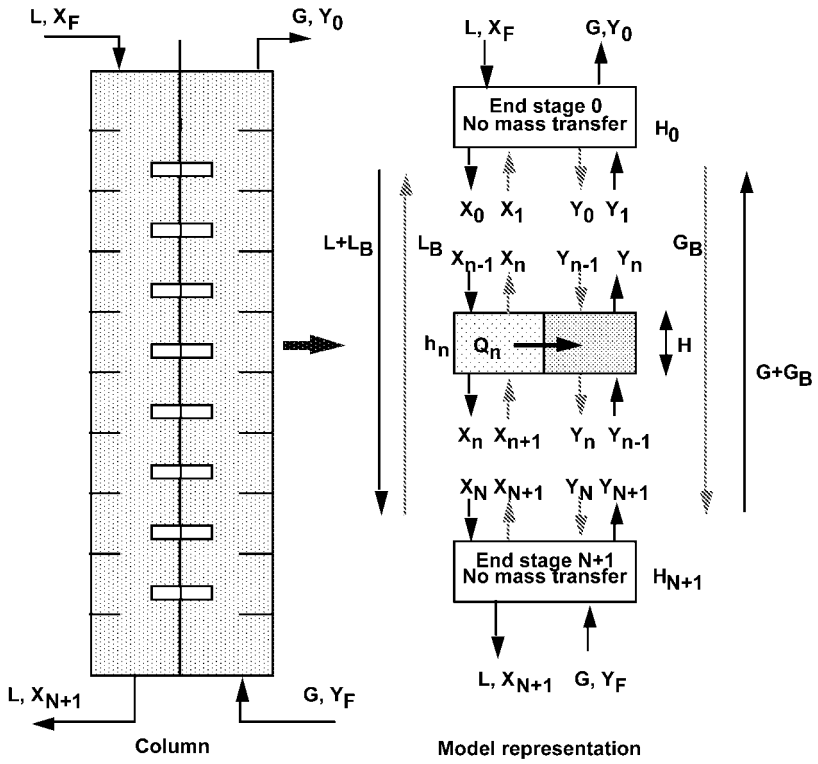

Fig. 3.47 Model representation of a non-equilibrium-staged extraction column.

in series and the constant backflow contributions, L_B and G_B, as indicated in Fig. 3.47 appropriate for each phase.

Special attention has to be given to the end compartments of an extraction column, since the phase inlet and outlet points are usually located at different points of the column. These are complicated by the presence of phase distributors and at one end by the coalescence zone for the dispersed phase droplets.

In Fig. 3.47 the end sections are represented quite simply as well-mixed zones, in which some limited degree of mass transfer may be present, but at which the mass transfer rate is much lower than in the main body of the column.

The standard equations for a stagewise extraction cascade with backmixing as developed in Section 3.3.1.5 are

$$V_{Ln}\frac{dX_n}{dt} = (L + L_B)(X_{n-1} - X_n) + L_B(X_{n+1} - X_n) - Q_n$$

$$V_{Gn}\frac{dY_n}{dt} = (G + G_B)(Y_{n+1} - Y_n) + G_B(Y_{n-1} - Y_n) + Q_n$$

where

$$Q_n = K_{Ln} a_n (X_n - X_n^*) V$$

and

$$X_n^* = f_{eq}(Y_n)$$

Here a_n is the interfacial area per unit volume.

In extraction column design the model equations are normally expressed in terms of superficial phase velocities, L′ and G′, based on unit cross-sectional area. The volume of any stage in the column is then A H, where A is the cross-sectional area of the column. Thus the volume occupied by the total dispersed phase is h A H, where h is the fractional holdup of dispersed phase, i.e., the droplet volume in the stage divided by the total volume of the stage. The volume occupied by the continuous phase in the stage is (1–h) A H.

Taking the phase flow rate G′ to represent the dispersed phase, the component balance equations now become for any stage n

$$A H_n (1 - h_n) \frac{dX_n}{dt} = (L' + L'_B)(X_{n-1} - X_n) + L'_B (X_{n+1} - X_n) - Q_n$$

$$A H_n h_n \frac{dY_n}{dt} = (G' + G'_B)(Y_{n+1} - Y_n) + G'_B (Y_{n-1} - Y_n) + Q_n$$

In the above equations K_L is the overall mass transfer coefficient (based on phase L), a is the specific interfacial area for mass transfer related to unit column volume, X and Y are the phase solute concentrations, X^* is the equilibrium concentration corresponding to concentration Y and subscript n refers to stage n of the extractor.

Normally the backmixing flow rates L_B and G_B are defined in terms of constant backmixing factors $\alpha_L = L_B/L$ and $\alpha_G = G_B/G$. The material balance equations then appear in the form

$$H_n (1 - h_n) \frac{dX_n}{dt} = L'(1 + \alpha_L) X_{n-1} - L'(1 + 2\alpha_L) X_n + \alpha_L L' X_{n+1} - Q_n$$

$$H_n h_n \frac{dY_n}{dt} = G'(1 + \alpha_G) Y_{n+1} - G'(1 + 2\alpha_G) Y_n + \alpha_G G' Y_{n-1} - Q_n$$

Considering the end regions of the column as well-mixed stages with small but finite rates of mass transfer, component balance equations can be derived for end stage 0

$$V_0 (1 - h_0) \frac{dX_0}{dt} = L X_F + L_B X_1 - (L + L_B) X_0 - Q_0$$

$$V_0 h_0 \frac{dY_0}{dt} = (G + G_B)(Y_1 - Y_0) + Q_0$$

and for end stage N

$$V_{N+1}(1 - h_{N+1})\frac{dX_{N+1}}{dt} = (L + L_B)(X_N - X_{N+1}) - Q_{N+1}$$

$$V_{N+1}h_{N+1}\frac{dY_{N+1}}{dt} = GY_F + G_BY_N - (G + G_B)Y_{N+1} + Q_{N+1}$$

The correct modelling of the end sections is obviously of great importance and, depending on the geometrical arrangement, it is possible to consider the column end sections as combinations of well-mixed tanks, exterior to the actual column.

3.3.1.11 Column Hydrodynamics

Under changing flow conditions it can be important to include some consideration of the hydrodynamic changes within the column (Fig. 3.48), as manifested by changes in the fractional dispersed phase holdup h_n and the phase flow rates L_n and G_n which, under dynamic conditions, can vary from stage to stage. Such variations can have a considerable effect on the overall dynamic characteristics of an extraction column, since variations in h_n also affect the solute transfer rate terms Q_n by virtue of the corresponding variation in the specific interfacial area a_n.

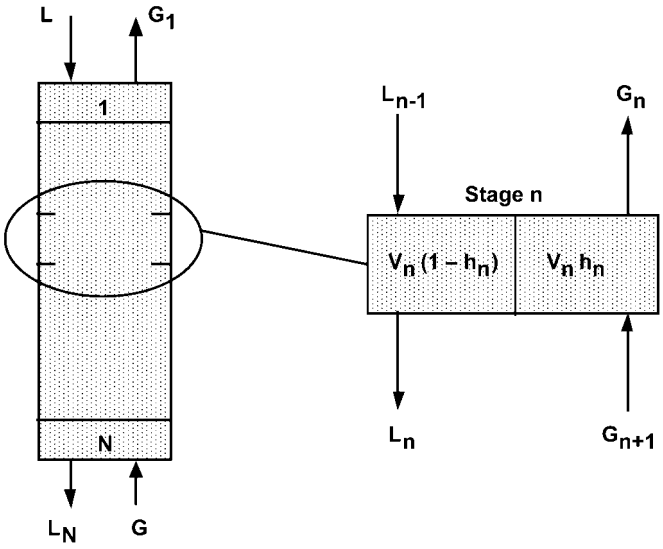

Fig. 3.48 Hydrodynamic model representation of an extraction column.

A dynamic balance for the dispersed phase holdup in stage n gives

$$V_n \frac{dh_n}{dt} = G_{n+1} - G_n$$

Since liquid phases are incompressible

$$L_{n-1} + G_{n+1} = L_n + G_n$$

and for the overall column

$$L + G = L_N + G_1$$

The fractional dispersed phase holdup h is normally correlated on the basis of a characteristic velocity equation, which is based on the concept of a slip velocity for the drops v_{slip}, which then can be related to the free rise velocity of single drops, using some correctional functional dependence on holdup f(h). The normal method of correlating dispersed phase holdup is normally of the form

$$v_{slip} = \frac{L'}{(1-h)} - \frac{G'}{h} = v_{char} f(h)$$

where v_{char} is the characteristic velocity for the dispersed phase droplets. Knowing the value of v_{char}, the value of h can be determined for any values of L′ and G′, using an iterative procedure.

In some cases, the characteristic velocity can cause difficulties in solution, owing to the presence of an implicit equation. In this the appropriate value of L_n or G_n satisfying the value of h_n generated by the differential material balance equation must be found by root finding algorithms increasing computation time required.

If necessary, the implicit nature of the calculation may, however, be avoided by a reformulation of the holdup relationship into an explicit form. The resulting calculation procedure then becomes much more straightforward and the variation of holdup in the column may be combined into a fuller extraction column model in which the inclusion of the hydrodynamics now provides additional flexibility. The above modelling approach to the column hydrodynamics, using an explicit form of holdup relationship, is illustrated by the simulation example HOLDUP.

3.3.2
Stagewise Absorption

Gas–liquid contacting systems can be modelled in a manner similar to liquid–liquid contactors. There are however some modelling features which are peculiar to gas–liquid systems. The single well-mixed contacting stage is shown in Fig. 3.49.

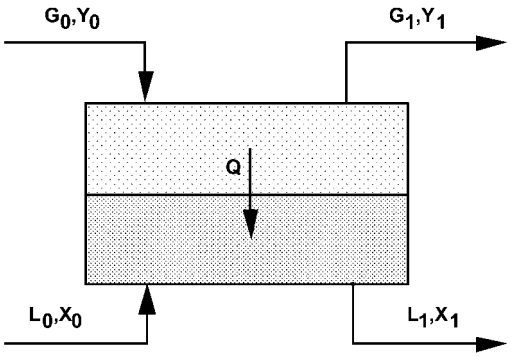

Fig. 3.49 Well-mixed gas–liquid contacting stage.

In this, G and L are the volumetric flow rates of the two phases, and X and Y are the concentrations of any component in each phase. Q is the transfer rate of the component.

For single-solute gas–liquid mass transfer the component balances are as before

$$V_L \frac{dX_1}{dt} = L_0X_0 - L_1X_1 + Q$$

$$V_G \frac{dY_1}{dt} = G_0Y_0 - G_1Y_1 - Q$$

where V_G is the volume of the well-mixed gas phase, and V_L is the volume of the well-mixed liquid phase.

In the preceding solvent extraction models, it was assumed that the phase flow rates L and G remained constant, which is consistent with a low degree of solute transfer relative to the total phase flow rate. For the case of gas absorption, normally the liquid flow is fairly constant and L_0 is approximately equal to L_1, but often the gas flow can change quite substantially, such that G_0 no longer equals G_1. For highly concentrated gas phase systems, it is therefore often preferable to define flow rates, L and G, on a solute-free mass basis and to express concentrations X and Y as mass ratio concentrations. This system of concentration units is used in the simulation example AMMONAB.

The transfer term Q is written as

$$Q = K_La(X_1^* - X_1)V_L$$

where a is the transfer surface per volume of liquid, K_L is the overall mass transfer coefficient for phase L, V_L is the liquid phase volume and X_1^* is given by the equilibrium relation

$$X_i^* = f_{eq}(Y_1)$$

As shown for the case of extraction, a high value of K_La will result in X_1 approaching very close to the value X_i^*, and therefore the outlet concentrations of the two phases will be close to equilibrium.

Owing to the substantially greater density of liquids, as compared to gases, the volumetric flow rate of the gas is usually much greater than that of the liquid or G >> L as a general consequence

$$\frac{V_L}{L} \gg \frac{V_G}{G}$$

meaning that

$$\tau_L \gg \tau_G$$

The significance of the large difference in the relative magnitudes of the time constants, for the two phases, is that the gas concentrations will reach steady state much faster than the liquid phase.

In the component balance equations dY_1/dt will therefore be zero, whereas dX_1/dt may still be quite large. This can obviously cause considerable difficulties in the integration procedure, owing to equation stiffness.

For gas absorption this problem can often be circumvented by the assumption of a quasi-steady-state condition for the gas phase. In this, the dynamics of the gas phase are effectively neglected and the steady state, rather than the dynamic form of component balance, is used to describe the variation in gas phase concentration.

The gas phase balance then becomes for the above situation

$$0 = G_0Y_0 - G_1Y_1 - Q$$

Hence

$$Y_1 = \frac{G_0Y_0 - K_La(X_1^* - X_1)V_L}{G_1}$$

Thus Y_1 is obtained not as the result of the numerical integration of a differential equation, but as the solution of an algebraic equation, which now requires an iterative procedure to determine the equilibrium value X_1^*. The solution of algebraic balance equations in combination with an equilibrium relation has again resulted in an implicit algebraic loop. Simplification of such problems, however, is always possible, when X_1^* is simply related to Y_1, as for example

$$X_1^* = mY_1$$

Combining the two equations then gives an explicit solution for concentration Y_1 and hence also X_1

$$Y_1 = \frac{G_0 Y_0 + K_L a X_1 V_L}{G_1 + K_L a m V_L}$$

and the implicit algebraic loop is eliminated from the solution procedure.

Assuming equilibrium conditions and a linear equilibrium relationship, where $Y_1 = m X_1$ and a quasi-steady-state conditions in the gas with $dY_1/dt = 0$ to be achieved, a component balance for the entire two phase system of Fig. 3.49 gives

$$V_L \frac{dX_1}{dt} = GY_0 + LX_0 - LX_1 - GmX_1$$

which can be expressed as

$$\frac{dX_1}{dt} = \frac{\frac{GY_0 + LX_0}{L + Gm} X_1}{\frac{V_L}{L + Gm}}$$

This equation has the form

$$\frac{dX_1}{dt} = \frac{A - X_1}{\tau}$$

where the time constant for the system, τ, is thus shown to be dependent on the value of the equilibrium constant m. Since the value of m depends on the nature of the particular solute concerned, this has the consequence that in multicomponent applications the value of the time constant will vary according to the system component. This can cause problems of equation stiffness in the solution of the often quite large sets of simultaneous multicomponent balance equations. The importance of eliminating unnecessary stiffness, by careful consideration of the relative magnitudes of the various system time constants, thus becomes very apparent.

3.3.3
Stagewise Distillation

3.3.3.1 Simple Overhead Distillation

A simple overhead topping distillation process, without fractionation, is illustrated in Fig. 3.50.

The total material balance is given by

$$\begin{pmatrix} \text{Rate of accumulation} \\ \text{of mass in the still} \end{pmatrix} = \begin{pmatrix} \text{Rate of mass} \\ \text{input to the still} \end{pmatrix}$$

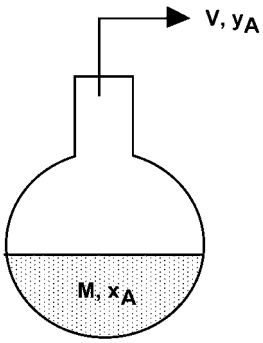

Fig. 3.50 Model representation of a simple overhead distillation.

giving

$$\frac{dM}{dt} = -V$$

where M is the total moles of liquid in the still and V is the vapour removal rate in moles/time.

For a simple binary distillation, the component balance equation becomes

$$\frac{d(Mx_A)}{dt} = -Vy_A$$

where x_A and y_A are the liquid and vapour mole fraction of component A of the liquid and vapour phases, respectively, where A is the more volatile component.

The relative volatility α is usually related to the compound having the higher boiling point, which in this case is B and hence

$$\alpha_{A/B} = \frac{y_A/x_A}{y_B/x_B}$$

Assuming that the liquid and vapour compositions in the still are in equilibrium, i.e., that the still acts as a theoretical stage

$$y_A = f_{eq}(x_A)$$

or in terms of relative volatility α

$$y_A = \frac{\alpha_A x_A}{1 + (\alpha_A - 1)x_A}$$

The combination of the two material balance equations, together with an explicit form of equilibrium relationship gives a system that is very easily solvable by direct numerical integration, as demonstrated in the simulation example BSTILL.

Extending the method to a multicomponent mixture, the total material balance remains the same, but separate component balance equations must now be written for each individual component i, giving

$$\frac{dMx_i}{dt} = -Vy_i$$

and where now the equilibrium condition is given by

$$y_i = \frac{\alpha_i x_i}{\Sigma \alpha_i x_i}$$

Again solution is straightforward, as illustrated in the simulation examples DIFDIST and MCSTILL.

3.3.3.2 **Binary Batch Distillation**

A batch distillation represents a complete dynamic process since everything, apart from the geometry of the column and the nature of the equilibrium relationship, varies with time. Owing to the removal of a distillate containing more of the volatile component, the compositions of the vapour and the liquid on all plates of the column vary with time. The total quantity of liquid in the still decreases with time, and its composition becomes successively depleted in the more volatile component. This makes the separation more and more difficult, requiring the use of higher reflux ratios to maintain a high distillate composition. The increased reflux increases the liquid flow down the column, and hence the liquid holdup on each plate. As a result of the increasing concentration of less volatile component in the still, the still temperature increases during distillation, thus reducing the rate of heat transfer to the still by reducing the temperature driving force in the reboiler and hence reducing the vapour boil-up rate. Despite this, conventional textbooks persist in analysing batch distillation in terms of quasi-steady-state graphical techniques applied at different concentration levels during the distillation process. These are also based on rather idealised and unrealistic conditions of operating a batch distillation process, i.e.:

1. Distillation at constant reflux ratio but varying top product composition.
2. Distillation at constant top product composition but varying reflux ratio.

Compared to this a solution approach based on digital simulation is much more realistic.

Consider the binary batch distillation column, represented in Fig. 3.51, and based on that of Luyben (1973, 1990). The still contains M_B moles with liquid mole fraction composition x_B. The liquid holdup on each plate n of the column is M_n with liquid composition x_n and a corresponding vapour phase composition y_n. The liquid flow from plate to plate L_n varies along the column with consequent variations in M_n. Overhead vapours are condensed in a total condenser and the condensate collected in a reflux drum with a liquid holdup volume M_D

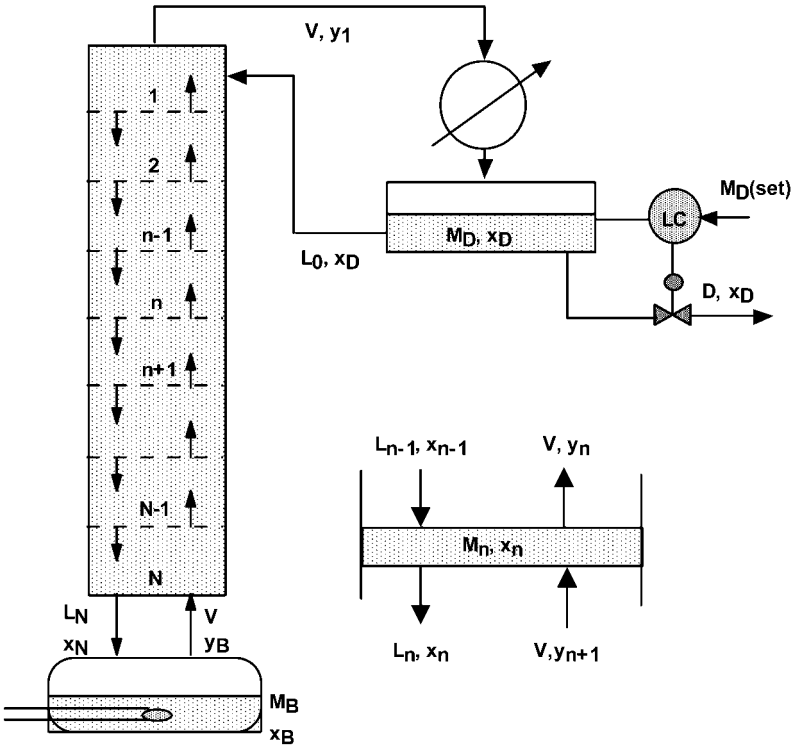

Fig. 3.51 Model representation of a batch distillation column and typical plate n as per Luyben (1973).

and liquid composition x_D. From here part of the condensate is returned to the top plate of the column as reflux at the rate L_0 and composition x_D. Product is removed from the reflux drum at a composition x_D and rate D, which is controlled by a simple proportional controller acting on the reflux drum level and is proportional to M_D.

For simplicity the following assumptions are made, although a more general model could easily be derived, in which these assumptions could be relaxed.

1. The system is ideal, with equilibrium described by a constant relative volatility, the liquid components have equal molar latent heats of evaporation and there are no heat losses or heat of mixing effects on the plates. Hence the concept of constant molar overflow (excluding dynamic effects) and the use of mole fraction compositions are allowable.
2. The liquid volumes in the still, reflux drum and on the column plates are well-mixed regions of uniform composition.
3. The dynamics of the overhead pipework and condenser are negligible.
4. The dynamics of the vapour phase in the column are much faster than that of the liquid phase and are neglected.

5. The still provides a constant vapour boil-up rate, which remains constant with respect to time.
6. The column plates have 100% plate efficiency and act as theoretical plates.

Since the vapour phase dynamics are negligible, the vapour flow rate through the column is constant from plate to plate, at the rate of V (kmol/s). The liquid flow rates L_n and the liquid holdup on the plate, however, will vary under changing hydrodynamic conditions in the column. The corresponding notation, for any plate n in the column, is as indicated in Fig. 3.51.

Total mass and component material balance equations are written for all the plates of the column, for the still and for the top reflux drum.

Here L, G and D are the molar flow rates and x and y are mol fraction compositions.

For plate n the total material balance is given by

$$\frac{dM_n}{dt} = L_{n-1} + V_{n+1} - L_n - V_n$$

Since vapour phase dynamics are neglected and "Constant Molal Overflow" conditions also apply, $V_{n+1} = V_n = V$, and

$$\frac{dM_n}{dt} = L_{n-1} - L_n$$

The component balance equation is given by

$$\frac{d(M_n x_n)}{dt} = L_{n-1}x_{n-1} - L_n x_n + V(y_{n+1} - y_n)$$

The corresponding equations for the boiler are

$$\frac{dM_B}{dt} = L_N - V$$

and

$$\frac{d(M_B x_B)}{dt} = L_N x_N - V y_B$$

where N refers to conditions on the bottom plate of the column.

For the reflux drum

$$\frac{dM_D}{dt} = V - D - L_0$$

and

$$\frac{d(M_D x_D)}{dt} = Y y_1 - (L_0 + D)x_D$$

where $L_0/D = R$ is the reflux ratio for the column.

Assuming theoretical plate behaviour, i.e., equilibrium between the gas and liquid phases, for plate n

$$y_n = \frac{\alpha x_n}{1 + (\alpha - 1)x_n}$$

where α is the relative volatility.

The above equation also applies to the liquid and vapour compositions of the still, where equilibrium plate behaviour is again assumed.

The maintenance of constant liquid level in the reflux drum can be expressed by the following proportional control equation

$$D = K_p(M_D - M_{D(set)})$$

where K_p is the controller gain and $M_{D(set)}$ is the level controller set point.

Automatic control of distillate composition (x_D) may also be affected by control of the reflux ratio, for example to maintain the distillate composition at constant set point (x_{Dset}).

$$R = K_{pR}(x_D - x_{Dset})$$

Batch distillation with continuous control of distillate composition via the regulation of reflux ratio is illustrated in the simulation example BSTILL. In this an initial total reflux condition, required to establish the initial concentration profile with the column, is represented in the simulation by a high initial value of R, which then changes to the controller equation for conditions of distillate removal.

Changes in the hydraulic hold-up of liquid on the column plates is known to have a significant effect on the separating efficiency of batch distillation columns, and may be relatively easily incorporated into the batch simulation model. The hydraulic condition of the plates is represented in Fig. 3.52.

A material balance for the liquid on plate n is given by

$$\frac{dM_n}{dt} = L_{n-1} - L_n$$

In this simplified model, it is assumed that liquid may leave the plate, either by flow over the weir $L_{n(weir)}$ or by weepage $L_{n(weep)}$. Both these effects can be described by simple hydraulic relations, in which the flow is proportional to the square root of the available hydrostatic liquid head. The weir flow depends on the liquid head above the weir, and hence

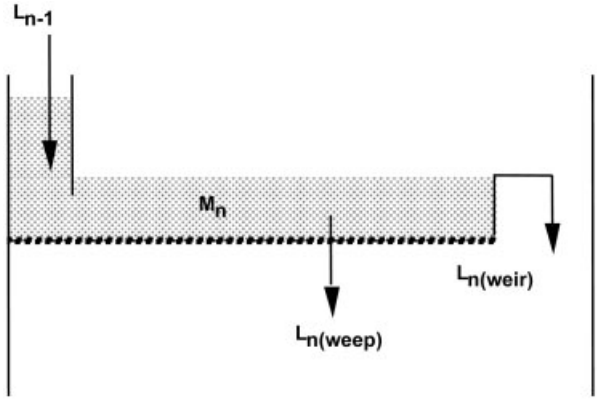

Fig. 3.52 Model representation of the plate hydraulics.

$$L_{n(weir)} \propto (M_n - M_{ns})^{0.5}$$

$L_{n(weir)}$ is zero for the condition $M_n < M_{ns}$. M_n is the mass of liquid on plate n, and M_{ns} is the mass of liquid on the plate corresponding to the weir height or static liquid holdup on the plate. The rate of loss of liquid from the plate by weepage, however, will depend on the total mass of liquid on the plate

$$L_{n(weep)} \propto M_n^{0.5}$$

The total flow of liquid from the plate is therefore given by

$$L_n = K_1(M_n - M_{ns})^{0.5} + K_2 M_n^{0.5}$$

where K_1 is an effective weir discharge constant for the plate, K_2 is the weepage discharge constant and M_{ns} is the static holdup on the plate.

3.3.3.3 **Continuous Binary Distillation**

The continuous binary distillation column of Fig. 3.53 follows the same general representation as that used previously in Fig. 3.51. The modelling approach again follows closely that of Luyben (1990).

The relationships for the section of column above the feed plate, i.e., the enriching section of the column, are exactly the same as those derived previously for the case of the batch distillation column.

The material balance relationships for the feed plate, the plates in the stripping section of the column and for the reboiler must, however, be modified, owing to the continuous feed to the column and the continuous withdrawal of bottom product from the reboiler. The feed is defined by its mass flow rate, F, its composition x_F and the thermal quality or q-factor, q. The column bottom prod-

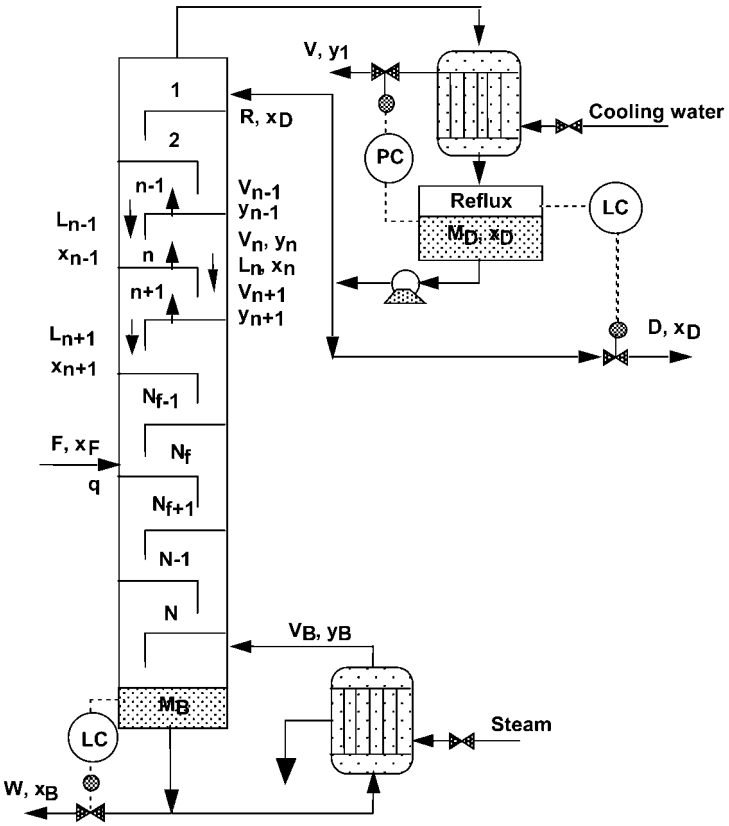

Fig. 3.53 Model representation of a continuous binary distillation column. PC is the cooling water controller, LC the reflux controller.

uct is defined by its mass flow rate W and composition x_W and is controlled to maintain constant liquid level in the reboiler.

The liquid and vapour molar flow rates in the enriching section are denoted by L and V, as previously and in the stripping section as L′ and V′. The relationship between L, V, L′ and V′ is determined by the feed rate F and the thermal quality of the feed "q".

The thermal quality of the feed is defined as the heat required to raise 1 mole of feed from the feed condition to vapour at the feed plate condition divided by the molar latent heat, and the following values apply: $q=0$ for saturated liquid feed; $q=1$ for saturated vapour feed, and $q>1$ for cold feed. The value of q affects the relative liquid and vapour flow rates (L and V) above and (L′ and V′) below the feed plate, as indicated in Fig. 3.54.

Thus an energy balance around the feed plate can be employed to show that under certain conditions

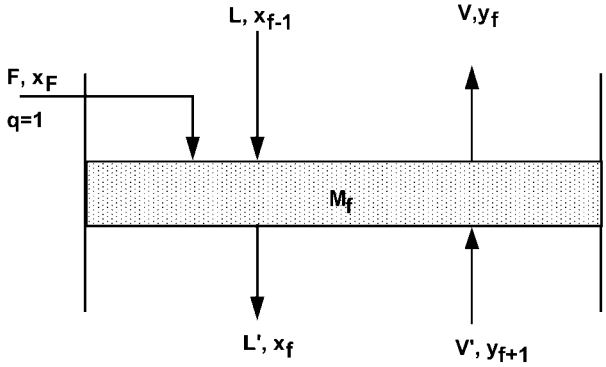

Fig. 3.54 Column feedplate flow rates and compositions.

$$L' = L + qF$$

$$V = V' - (1 - q)F$$

and where for a saturated liquid feed with q=1

$$L' = L + F$$

and

$$V = V'$$

For any plate n above the feed as shown previously for constant liquid holdup conditions

$$M_n \frac{dx_n}{dt} = L(x_{n-1} - x_n) + V(y_{n+1} - y_n)$$

The component balance for the feed plate is given by

$$M_n \frac{dx_F}{dt} = Lx_{f-1} - L'x_f + V'y_{F+1} - Vy_f + Fx_F$$

and for any plate m, in the stripping section, below the feed

$$M_m \frac{dx_n}{dt} = L'(x_{m-1} - x_m) + V'(y_{m+1} - y_m)$$

For the reboiler

$$M_B \frac{dx_B}{dt} = L'x_N - Wx_B - V'y_B$$

The controller equations

$$W = f(M_B)$$

$$V' = f(x_B)$$

are also required to complete the model. The relationships around the top part of the column and control of reflux drum level remain the same as those for the batch situation, described in Section 3.3.3.2.

If necessary the hydraulic relationships, previously derived for batch distillation, are also easily implemented into a continuous distillation model.

Continuous binary distillation is illustrated by the simulation example CONSTILL. Here the dynamic simulation example is seen as a valuable adjunct to steady state design calculations, since with MADONNA the most important column design parameters (total column plate number, feed plate location and reflux ratio) come under the direct control of the simulator as facilitated by the use of sliders. Provided that sufficient simulation time is allowed for the column conditions to reach steady state, the resultant steady state profiles of composition versus plate number are easily obtained. In this way, the effects of changes in reflux ratio or choice of the optimum plate location on the resultant steady state profiles become almost immediately apparent.

3.3.3.4 **Multicomponent Separations**

As discussed previously in Section 3.3.1.7, each additional component of the feed mixture must be expressed by a separate component material balance equation and by its own equilibrium relationship.

Thus for component i of a system of j components, the component balance equation, on the nth plate, becomes

$$M_n \frac{dx_{in}}{dt} = L(x_{in-1} - x_{in}) + V(y_{in+1} - y_{in})$$

where i=1 to j.

Assuming the equilibrium to be expressed in terms of relative volatilities a_i and theoretical plate behaviour, the relation between the vapour and liquid mole fraction compositions leaving the plate is given by

$$y_{in} = \frac{a_{in}x_{in}}{\sum_{1}^{j} a_{in}x_{in}}$$

or where the equilibrium can be based in terms of K values, the relationship becomes

$$y_{in} = K_{in}x_{in}$$

Using the above form of equilibrium relationship, the component balance equations now become

$$M_n \frac{dx_{in}}{dt} = Lx_{in-1} - Lx_{in} + VK_{in}(x_{in+1} - x_{in})$$

This again shows that the component balance may thus have different time constants, which depend on the relative magnitudes of the equilibrium constants K_i, which again can lead to problems of numerical solution due to equation stiffness.

One way of dealing with this is to replace those component balance differential equations, having low time constants (i.e., high K values) and fast rates of response, by quasi-steady-state algebraic equations, obtained by setting

$$M \frac{dx_i}{dt} = 0$$

and effectively neglecting the dynamics in the case of those components, having very fast rates of response.

Continuous multicomponent distillation simulation is illustrated by the simulation example MCSTILL, where the parametric runs facility of MADONNA provides a valuable means of assessing the effect of each parameter on the final steady state. It is thus possible to rapidly obtain the optimum steady state settings for total plate number, feed plate number and column reflux ratio via a simple use of sliders.

3.3.3.5 **Plate Efficiency**

The use of a plate efficiency correction enables the simulation of columns with a real number of plates to be simulated. This may be important in the study of real columns, when incorporating an allowance for plate hydrodynamic behaviour.

The situation for any plate n, with liquid composition x_n corresponding to an equilibrium vapour composition y_n^*, but with actual vapour composition y_n, is represented on a small section of the McCabe–Thiele diagram in Fig. 3.55.

The actual plate efficiency can be defined as

$$\eta = \frac{\text{Actual change of composition}}{\text{Maximum possible change of composition}}$$

where

$$\eta = \frac{(y_n - y_{n1})}{(y_n^* - y_{n1})}$$

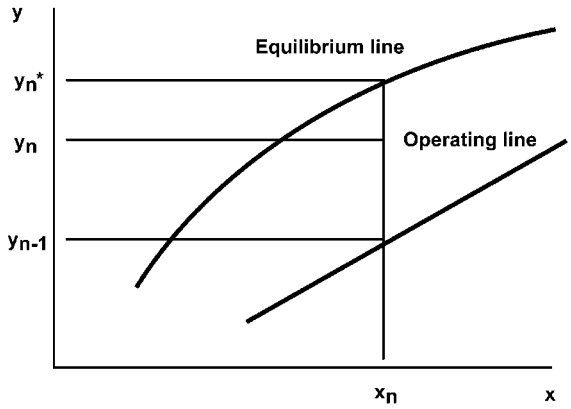

Fig. 3.55 Actual and theoretical plate compositions for plate n.

Hence by simple algebra

$$y_n = \eta(y_n^* - y_{n-1}) + y_{n-1}$$

Additional equations, as above, can thus be used to correct the values of y_n^*, obtained from the equilibrium data to give actual plate values y_n.

3.3.3.6 **Complex Column Simulations**

More complex situations where ideal behaviour can no longer be assumed require the incorporation of activity coefficient terms in the calculation of the equilibrium vapour compositions. Assuming ideal behaviour in the gas phase, the equilibrium relation for component i is

$$y_i = \frac{\gamma_i x_i P_i}{P}$$

where P is the total pressure in the column. Since the saturated vapour pressure of the pure compound i, P_i, is a function of temperature, the calculation of the equilibrium vapour composition requires that a plate temperature must be determined such that the condition $\Sigma y_i = 1$ is obtained. Examples of this technique are illustrated in the corresponding simulation examples STEAM and BUBBLE.

Furthermore heat effects on the plates may also have to be accounted for, by means of a dynamic heat balance for each plate, including allowances for the enthalpies of the liquid and vapour streams, entering and leaving the plate, heat of mixing, etc. This thus represents a much more complicated and time-consuming computational procedure than has been considered so far. In such cases, it obviously becomes much more meaningful to employ larger simulation packages, with their sophisticated physical property data-bases and estimation

procedures. The general principles of the modelling procedure, however, remain very much the same.

Multicomponent equilibria combined with distillation heat effects are discussed in more detail in Section 3.3.4 below.

3.3.4
Multicomponent Steam Distillation

Steam distillation is a process whereby organic liquids may be separated at temperatures sufficiently low to prevent their thermal decomposition or whereby azeotropes may be broken. Fats or perfume production are examples of applications of this technique. The vapour–liquid equilibria of the three-phase system is simplified by the usual assumption of complete immiscibility of the liquid phases and by the validity of the Raoult and Dalton laws. Systems containing more than one volatile component are characterised by complex dynamics (e.g., boiling point is not constant).

Steam distillation is normally carried out as a semi-batch process whereby the organic mixture is charged into the still and steam is bubbled through continuously, as depicted in Fig. 3.56.

As discussed, modelled and simulated by Prenosil (1976), the dynamics of the process bring in the question of steam consumption, steam flow rate, starting time of the distillation, and shut-down time when the desired degree of separation has been reached. The modelling of steam distillation often involves the following assumptions.

1. Ideal behaviour of all components in pure state or mixture.
2. Complete immiscibility of the water and the organic phases.
3. Zero temperature gradients in the bulk phases (ideal mixing in the boiler).
4. Equilibrium between the organic vapour and its liquid at all times.

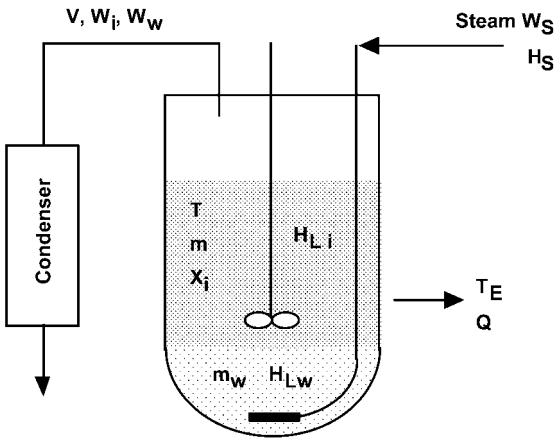

Fig. 3.56 Schematic drawing of the apparatus for steam distillation.

The mathematical model is divided into two time periods:

(a) The heating period until boiling point is reached.
(b) The distillation period after boiling has started.

Heating Period

To describe the dynamic behaviour of this semi-batch process, unsteady-state mass and energy balances are needed. Their interrelationships are depicted in Fig. 3.57.

For the water phase,

$$\frac{dm_w}{dt} = W_S$$

Here, it is assumed that all the steam condenses in the distillation vessel. In this period, the organic phase component masses remain constant.

The rate of heat accumulation is balanced by the heat of condensation and the heat losses. An energy balance therefore gives

$$\frac{d(m_w H_{Lw} + m\Sigma x_i H_{Li})}{dt} = W_S H_S + Q$$

The enthalpy changes are calculated from molar heat capacities given by the usual functions of temperature, according to

$$(m_w c_{pLw} + m\Sigma x_i c_{pLi})\frac{dT}{dt} = W_S(H_S - H_{Lw}) + Q$$

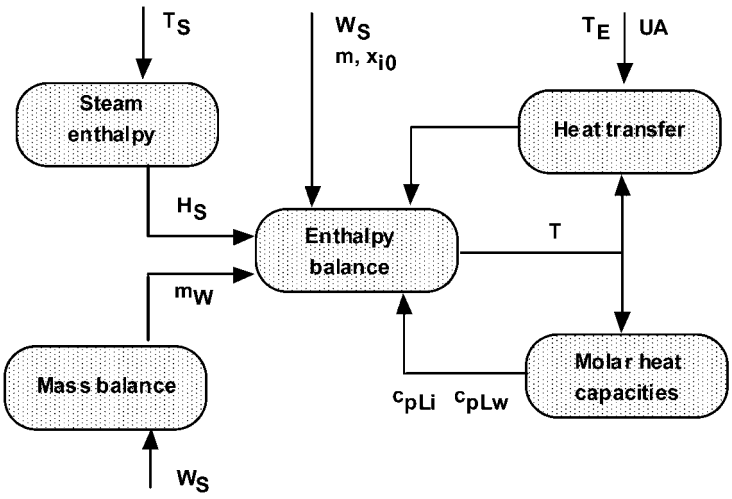

Fig. 3.57 Information flow diagram for the heating period.

from which it follows that

$$\frac{dT}{dt} = \frac{W_S(H_S - H_{Lw}) + Q}{m_w c_{pLw} + \Sigma x_i c_{pLi}}$$

The heat transfer Q to the surroundings is calculated from the simple relation

$$Q = UA(T_E - T)$$

The solution of the above model gives the temperature of the mixture at any time during the heating period.

Distillation Period

The distillation starts when the boiling point is reached. Then a vapour stream at flow rate V is obtained, which condenses as a distillate. The material balances can be written as follows:

For water

$$\frac{dm_w}{dt} = W_S - Vy_v$$

For the organic compound i

$$\frac{d(mx_i)}{dt} = -Vy_i$$

and for the total organic phase

$$\frac{dm}{dt} = -V\Sigma y_i$$

The energy balance is now

$$\frac{d(m_w H_{Lw} + m\Sigma x_i H_{Li})}{dt} = W_S H_S - VH_V + Q$$

where

$$H_V = y_w H_{Vw} + \Sigma y_i H_{Vi}$$

The vapour enthalpies are calculated from the molar heat capacity functions for the vapour components and the latent heats of vaporisation at standard temperature. The vapour overflow, V, is then obtained from the energy balance as

$$V = W_S H_S + Q - \frac{d(m_w H_{Lw} + m\Sigma x_i H_{Li})}{dt}\frac{1}{H_V}$$

Phase Equilibria

Assuming ideal liquid behavior, the total partial pressure of the organic phase is given by the sum of the partial pressures of its components according to Raoult's Law.

$$\frac{y_i}{x_i} = \frac{P_i}{P}$$

where P_i is the vapour pressure of pure component i. For non-idealities, this must be modified with appropriate activity expressions (Prenosil, 1976). For water, the vapour pressure varies only with temperature so that

$$y_w = \frac{P_w}{P}$$

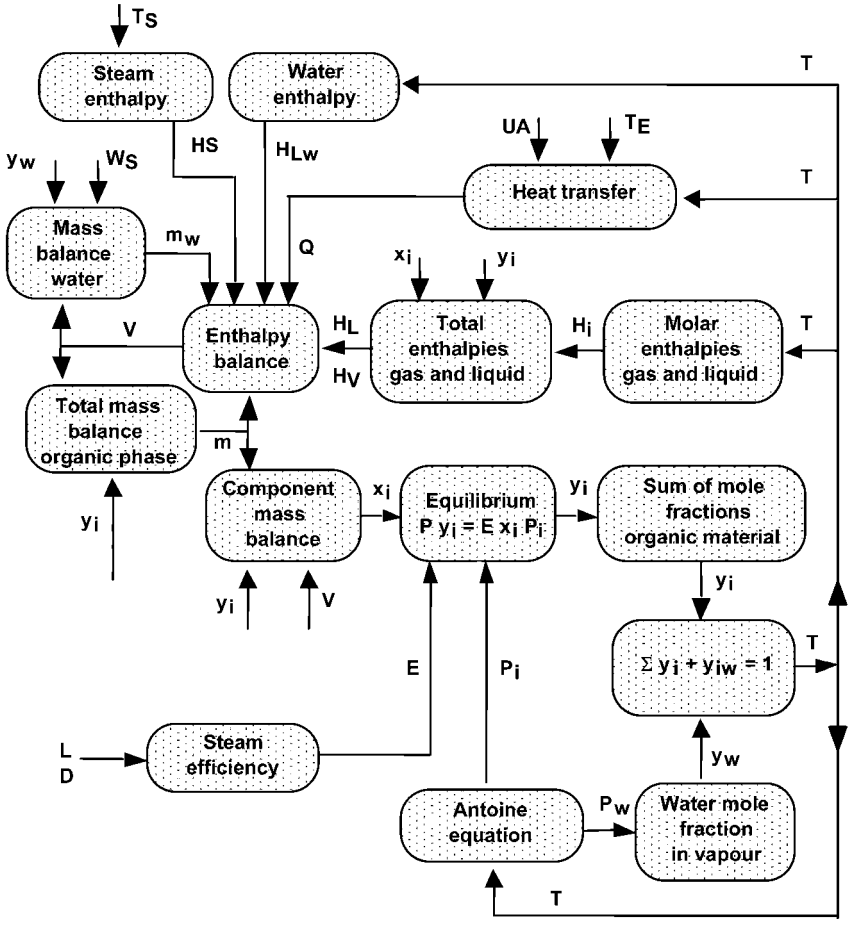

Fig. 3.58 Information flow diagram for the distillation period.

Boiling will commence when the sum of the organic partial pressures and the water vapour pressure is equal to the total pressure or in terms of the mole fractions

$$\Sigma y_i + y_w = 1$$

As boiling proceeds the loss of the lightest organic vapours will cause the boiling point to increase with time. The vapour pressures P_i and P_w of the pure components can be calculated using the Antoine equation

$$\log P = A - \frac{B}{C + T}$$

The highly interactive nature of the balance and equilibria equations for the distillation period are depicted in Fig. 3.58. An implicit iterative algebraic loop is involved in the calculation of the boiling point temperature at each time interval. This involves guessing the temperature and calculating the sum of the partial pressures or mole fractions. The condition required is that $\Sigma y_i + y_w = 1$. The model of Prenosil (1976) also included an efficiency term E for the steam heating, dependent on liquid depth L and bubble diameter D.

Multicomponent steam distillation is illustrated in simulation example STEAM.